JOURNAL OF COMPUTATIONAL PHYSICS **123,** 45–64 (1996)
ARTICLE NO. 0004

Stable Conservative Multidomain Treatments for Implicit Euler Solvers

A. LERAT AND Z. N. WU

SINUMEF Laboratory, Ecole Nationale Supérieure d'Arts et Métiers
151 bd de l'Hôpital, 75013 Paris, France

Received February 7, 1994; revised April 19, 1995

Multidomain treatments are studied in order to solve the steady compressible Euler equations using implicit time-dependent finite volume methods on block-structured grids. Unconditionally GKS-stable and conservative treatments are proposed for continuous and discontinuous 1D matchings and extended to 2D patched grids. Efficiency of the present interface conditions is demonstrated through transonic flow calculations over single- and two-element airfoils. © 1996 Academic Press, Inc.

1. INTRODUCTION

In computational fluid dynamics, the domain decomposition technique is now widely used to deal with complex flow geometries. This technique makes the distribution of the mesh points easier, reduces the size of the algebraic problems to be solved, and allows for an efficient use of parallel computers [22].

In the subdomains, one can use either a structured or an unstructured mesh. Unstructured meshes generally lead to more sophisticated and time-consuming methods per mesh point, but they allow for optimal distribution of mesh points and are very flexible for practical applications (see, for instance, [1, 13, 19, 21, 30]). On the other hand, structured meshes lend themselves more easily to high accuracy and simplify the structure of the algebraic systems. Non-body-fitted Cartesian grids have also been studied (see, for instance, [10, 32, 33, 38]). They undoubtedly provide the most accurate methods for the flow regions away from the solid boundaries, but they require a special treatment for the solid boundaries.

In the present paper, we study the multidomain technique using structured body-fitted grids for calculating steady solutions of hyperbolic systems of conservation laws. The equations are solved by implicit time-dependent finite-volume methods. At the interface of two adjacent subdomains, the solutions are matched by some *interface* or *matching conditions.* The difficulty here is to define these interface conditions so that the global approximation is spatially accurate, GKS-stable (i.e., stable in the sense of Gustafsson, Kreiss, and Sundström [18]), conservative, and converges to a steady-state.

Previous studies of interface conditions satisfying one or more of the above criteria for various applications have concentrated mainly on explicit difference schemes. Ciment [8, 9] studied the matching of dissipative schemes with or without mesh refinement. Browning, Kreiss, and Oliger [6] analyzed a mesh refinement technique with the non-dissipative leap-frog scheme. Starius [43] considered composite-mesh methods for accurately treating curvilinear boundaries. Oliger [34] examined a hybrid difference method in order to treat the boundary condition for a high-order difference scheme in a stable way. Berger considered the stability of mesh refinement in space and time [4] and proposed a procedure to derive conservative difference approximations at grid interfaces for one- or two-dimensional arbitrarily overlapping grids [5]. Thuné [46] offered some general stability results for approximations of hyperbolic systems on substructured domains. Rai [41] devised a conservative interface treatment for patched grids having a common cell-center line. Chesshire and Henshaw [7] studied interface conditions for composite overlapping grids with emphasis on the accuracy. Enander [12] analyzed the stability of a patching procedure. Pärt and Sjögreen [39, 40] analyzed the stability of Berger's conservative flux interpolation method for the Lax–Wendroff scheme and applied the reconstruction method to derive stable and nearly conservative interface conditions. Steger and Benek [44] reviewed some of the advantages and difficulties of using various composite-grid schemes. Gustafsson [17] recently reported some theoretical and numerical results about the solution of the Euler and Navier–Stokes equations on patched and overlapping grids. The matching of different differential equations was also considered in [17].

Multidomain treatment with implicit schemes is a more difficult task because at each time step all the discrete unknowns are spatially coupled. The key point is the choice of interface conditions that allow for independent and stable solution of difference equations in each subdomain. This does not seem to have been analyzed in any depth in the past for hyperbolic problems. Despite this, successful computations have been reported. For example, Rai [42] devised an iterative procedure at each time step to match the second-order Osher scheme using

0021-9991/96 $12.00

his patched grid technique developed in [41]. Another example is given by Baysal, Fouladi, and Lessard [2] who applied an implicit upwind scheme, combined with a multigrid approach on overlapping and embedded grids. In both of the above examples, some matrix elements associated with the interface values are dropped to zero in the implicit system to uncouple the difference equations in each subdomain.

In the present paper, a multidomain technique is considered for dissipative implicit schemes and various interface configurations such as matchings with and without mesh refinement and patched grids. Stable and conservative interface conditions are proposed. The present interface conditions are inexpensive and convenient for parallel computing. They require no grid overlapping or iteration at each time step to be unconditionally GKS-stable and they lead to uncoupled solution of the interior implicit schemes. The idea for constructing these interface conditions is simply to lag in time the interface values that depend on the adjacent grid. This time lagging does not degrade the stability of the interior implicit schemes, provided it is correctly done.[1] The time lagging may degrade the convergence rate for obtaining the steady-state solution (see [52] for a convergence study). In our present calculations, this convergence loss has been found to be quite small (see Section 7.2).

The remainder of this paper is organized as follows. In Section 2, the difference approximation is first formulated for a one-dimensional hyperbolic problem on the strip $-1 < x < 1$ containing two subgrids and then reduced to a convenient form for stability analysis. The GKS theory is briefly recalled in order to analyze the stability of the interface problem. Some important properties of dissipative difference schemes are discussed. In order to show later on that our interface treatment, which is stable for dissipative difference schemes, remains sometimes, but not always, stable for nondissipative schemes, a class of schemes based on a linear multistep method in time and a centred difference in space is also briefly discussed. In Section 3, matching conditions for several easily workable 1D interface configurations are presented and their GKS-stability is analyzed. In Section 4, conservation of interface conditions for nonlinear conservation laws is addressed. First, the conservation of the interface conditions discussed in Section 3 is analyzed by using the Berger's conservation criterion [5]. In case of no conservation a conservative treatment is presented. In Section 5, multidimensional stability is considered and the universal artificial stabilizing technique of Michelson [31] is discussed for domain decomposition. In Section 6, a stable conservative interface treatment is proposed for patched grids. The patched grid we consider has a common cell-side line at the interface and thus is different from the one treated by Rai [42] and Enander [12]. Finally in Section 7, applications to the 2D Euler equations are presented. Various external flows over a NACA0012 airfoil and a two-element airfoil are computed using the stable implicit multidomain technique.

[1] Preliminary results of this study have been presented in [29] and heuristically extended to the Navier–Stokes equations in [23].

2. ONE-DIMENSIONAL INTERFACE PROBLEM AND GKS-STABILITY THEORY

In this section, we first formulate the interface problem for a linear one-dimensional problem using general multilevel three-point difference schemes and then state some basic results for later stability analysis using the GKS-theory.

2.1. *Formulation of the Interface Problem*

We consider the linear hyperbolic system:

$$W_t + AW_x = 0, \quad -1 < x < 1,\ t > 0, \tag{1}$$

where $W(x, t) \in \mathbf{R}^m$ and A is a constant non-singular $m \times m$ matrix having m real eigenvalues and a complete set of eigenvectors. Without loss of generality, we suppose that A is of diagonal form and partioned as $A = \mathrm{diag}(A^{\mathrm{I}}, A^{\mathrm{II}})$, $A^{\mathrm{I}} > 0$, $A^{\mathrm{II}} < 0$.

The system (1) is completed by the initial condition

$$W(x, 0) = f(x), \quad -1 < x < 1, \tag{2}$$

and boundary conditions

$$W^{\mathrm{I}}(-1, t) = S^{\mathrm{I}} W^{\mathrm{II}}(-1, t) + g_{-1}(t), \quad t \geq 0, \tag{3}$$

$$W^{\mathrm{II}}(1, t) = S^{\mathrm{II}} W^{\mathrm{I}}(1, t) + g_1(t), \quad t \geq 0, \tag{4}$$

where W^{I} and W^{II} correspond to the partition of A and S^{I} and S^{II} are real rectangular matrices.

For the numerical solution of this initial-boundary value problem, the spatial domain $-1 \leq x \leq 1$ is split into two subdomains $\mathcal{D}_u = [-1, 0]$ and $\mathcal{D}_v = [0, 1]$. The subdomain D_u (resp. D_v) is divided into cells of equal length $\Delta x^{(u)}$ (resp. $\Delta x^{(v)}$) centred at $x = x_j^{(u)}$ (resp. $x_j^{(v)}$). For the location of these cells with respect to the *interface* $x = 0$, we assume that there is a cell of D_u and a cell of D_v having either a common side at the interface (*matching of first kind*) or a common center at the interface (*matching of second kind*). Furthermore, a matching is said to be *continuous* if $\Delta x^{(u)} = \Delta x^{(v)}$ or *discontinuous* if not.

For convenience, the cells are numbered from right to left in D_u and from left to right in D_v. The numerical solutions in the subdomains are denoted by

$$U_j^n \approx W(x_j^{(u)}, n\,\Delta t), \quad j = 0, 1, \ldots, N_u + 1,$$

$$V_j^n \approx W(x_j^{(v)}, n\,\Delta t), \quad j = 0, 1, \ldots, N_v + 1,$$

where Δt is the time step.

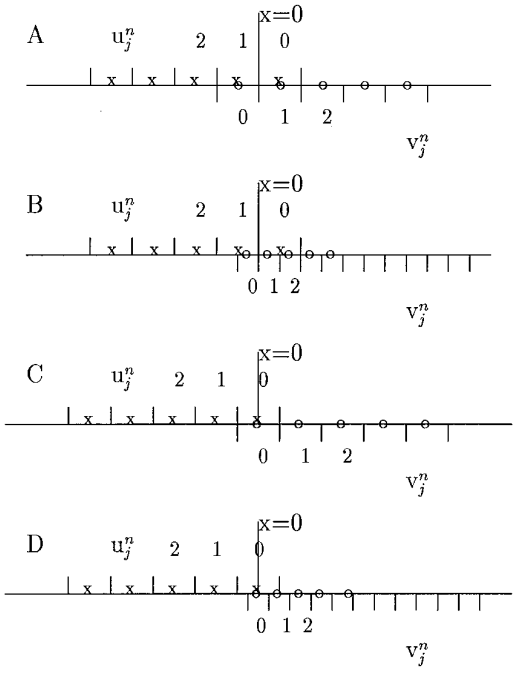

FIG. 1. (A) Continuous matching of first kind. (B) Discontinuous matching of first kind. (C) Continuous matching of second kind. (D) Discontinuous matching of second kind. Symbol ×: cell centers in the left subdomain. Symbol ○: cell centers in the right subdomain.

For a matching of first kind (see Fig. 1A for continuous matching and Fig. 1B for discontinuous matching), the interface is located between the cells $j = 0$ and $j = 1$ in each subdomain so that $\Delta x^{(u)} = 1/N_u$, $x_j^{(u)} = -(j - 1/2)\,\Delta x^{(u)}$ and $\Delta x^{(v)} = 1/N_v$, $x_j^{(v)} = (j - 1/2)\,\Delta x^{(v)}$. For a matching of second kind (see Fig. 1C for continuous matching and Fig. 1D for discontinuous matching), the interface is located at the cell center $j = 0$ in each subdomain so that $\Delta x^{(u)} = 1/(N_u + 1)$, $x_j^{(u)} = -j\,\Delta x^{(u)}$ and $\Delta x^{(v)} = 1/(N_v + 1)$, $x_j^{(v)} = j\,\Delta x^{(v)}$.

In each subdomain the problem (1)–(4) is approximated by implicit difference schemes with $2 + s$ time levels and 3 points in space:

$$\sum_{p=-1}^{1} B_p^{(u)} U_{j+p}^{n+1} = \sum_{q=0}^{s} \sum_{p=-1}^{1} C_{p,q}^{(u)} U_{j+p}^{n-q}, \quad j = 1, 2, ..., N_u, \tag{5}$$

$$U_{N_u+1}^{n+1} = \sum_{q=-1}^{s} S_q^{\mathrm{I}} U_{N_u}^{n-q} + g_{-1}^{n+1} \tag{6}$$

$$U_j^0 = f(-x_j), \quad j = 1, 2, ..., N_u, \tag{7}$$

$$\sum_{p=-1}^{1} B_p^{(v)} V_{j+p}^{n+1} = \sum_{q=0}^{s} \sum_{p=-1}^{p=1} C_{p,q}^{(v)} V_{j+p}^{n-q}, \quad j = 1, 2, ..., N_v, \tag{8}$$

$$V_{N_v+1}^{n+1} = \sum_{q=-1}^{s} S_q^{\mathrm{II}} V_{N_v}^{n-q} + g_{+1}^{n+1} \tag{9}$$

$$V_j^0 = f(x_j), \quad j = 1, 2, ..., N_v, \tag{10}$$

where $B_p^{(u)}$, $C_{p,q}^{(u)}$, $B_p^{(v)}$, and $C_{p,q}^{(v)}$ are diagonal $m \times m$ matrices, S^{I} and S^{II} are rectangular matrices and s is some non-negative integer.

At the interface $x = 0$, the two solutions are matched by an *interface condition* involving $2 + s$ time levels and l points in space,

$$\begin{aligned} U_0^{n+1} &= \sum_{q=-1}^{s} \sum_{p=1}^{l} (d_{p,q}^{(u,u)} U_p^{n-q} + d_{p,q}^{(u,v)} V_p^{n-q}) \\ V_0^{n+1} &= \sum_{q=-1}^{s} \sum_{p=1}^{l} (d_{p,q}^{(v,v)} V_p^{n-q} + d_{p,q}^{(v,u)} U_p^{n-q}), \end{aligned} \tag{11}$$

where $d_{p,q}^{(u,u)}$, $d_{p,q}^{(u,v)}$, $d_{p,q}^{(v,v)}$, and $d_{p,q}^{(v,u)}$ are scalar coefficients.

2.2. *GKS-Theory Applied to the Interface Problem*

The GKS-theory (Gustafsson, Kreiss, and Sundström [18]) is a general stability theory for mixed initial-boundary value problems. It is based on normal mode analysis. The *normal mode analysis* was developed by several authors, notably Kreiss [25, 26], Osher [35, 36], and Gustafsson, Kreiss, and Sundström [18]. Further work related to normal mode analysis has been carried out by Osher [37] and Varah [51] for parabolic problems, by Strikwerda [45] for semidiscretized equations, and by Michelson [31] for multidimensional strictly hyperbolic problems. Other contributions are due to Goldberg and Tadmor [14, 15] who constructed scheme-independent stability criteria for translatory boundary conditions, and also to Trefethen who physically interpreted the GKS-theory [48] and examined new instabilities in problems with multiple boundaries and interfaces [49, 50].

The stability of an interface problem can be analyzed by introducing the *folding trick* of Ciment [8, 9]. This trick consists in folding the left subdomain over the right one, thus transforming the interface problem into an equivalent right half-problem for which the GKS-theory is directly applicable. Our special numbering in the left subdomain (the cells are numbered from right to left) introduces the folding trick in a natural way.

A GKS-stable approximation subjected to a small perturbation remains stable, so that the stability of a multiinterface problem follows from that of each individual interface subproblem (see, for instance, [46]). Since one of the purposes of this paper is to study the stability of interface treatments but not that of boundary conditions, we assume that each exterior boundary treatment is stable and consider only the stability of the *Cauchy problem with interface* defined by the initial value problems (5), (7) for $j = 1, 2, ...$ ($x < 0$), and (8), (10) for $j = 1, 2, ...$ ($x > 0$) connected by interface condition (11) at $x = 0$. Since this problem is in diagonal form and the interface condition (11) involves only scalar coefficients, it is sufficient to consider the stability of the *reduced interface problem* defined by the

Cauchy problem with interface for the scalar equation $w_t + aw_x = 0$ with $a \neq 0$. In the scalar case, (5)–(8) can be written as

$$\sum_{p=-1}^{1} b_p^{(u)} u_{j+p}^{n+1} = \sum_{q=0}^{s} \sum_{p=-1}^{1} c_{p,q}^{(u)} u_{j+p}^{n-q}, \quad j = 1, 2, ..., \tag{12}$$

$$\sum_{p=-1}^{1} b_p^{(v)} v_{j+p}^{n+1} = \sum_{q=0}^{s} \sum_{p=-1}^{1} c_{p,q}^{(v)} v_{j+p}^{n-q}, \quad j = 1, 2, ..., \tag{13}$$

and the interface condition (11) becomes

$$\begin{aligned} u_0^{n+1} &= \sum_{q=-1}^{s} \sum_{p=1}^{m} (d_{p,q}^{(u,u)} u_p^{n-q} + d_{p,q}^{(u,v)} v_p^{n-q}) \\ v_0^{n+1} &= \sum_{q=-1}^{s} \sum_{p=1}^{m} (d_{p,q}^{(v,v)} v_p^{n-q} + d_{p,q}^{(v,u)} u_p^{n-q}). \end{aligned} \tag{14}$$

To analyze the GKS-stability of the reduced interface problem, we look for *normal mode solutions* of the form

$$u_j^n = z^n \phi_j^{(u)}, \quad v_j^n = z^n \phi_j^{(v)}, \quad j \in \mathbf{N}, \tag{15}$$

where $z \in \mathbf{C}$ and $\phi^{(u)}$, $\phi^{(v)}$ are l_2-solutions of the resolvent equations obtained by inserting the normal mode solution (15) into (12)–(13). In the present case, $\phi_j^{(u)} = \kappa_u^j u_0$ and $\phi_j^{(v)} = \kappa_v^j v_0$, where κ_u and κ_v are roots of the following characteristic equations of schemes (12) and (13):

$$\sum_{p=-1}^{1} b_p^{(u)} z \kappa_u^p = \sum_{q=0}^{s} \sum_{p=-1}^{1} c_{p,q}^{(u)} z^{n-q} \kappa_u^p \tag{16}$$

$$\sum_{p=-1}^{1} b_p^{(v)} z \kappa_v^p = \sum_{q=0}^{s} \sum_{p=-1}^{1} c_{p,q}^{(v)} z^{n-q} \kappa_v^p. \tag{17}$$

For any z with $|z| > 1$, the characteristic equation (16) has one root $|\kappa_u| < 1$ (called the *inner root*) and one root $|\kappa_u| > 1$ (called the *outer root*). The same is true for Eq. (17). For $\phi^{(u)}$ (resp. $\phi^{(v)}$) to be in l_2, κ_u (resp. κ_v) should be the inner root.[2] When $|z| = 1$, one or both of the roots of each characteristic equation may have modulus equal to one. If this is the case, the inner root for $|z| = 1$ is defined by continuity as the limit of the inner root for $|z| > 1$ as $|z| \to 1$ and the normal mode solution no longer belongs to l_2, but is a limit of l_2 solutions.

A necessary and sufficient condition for the reduced interface problem to be GKS-stable is that there are no nontrivial solutions of the form (15) with $|z| \geq 1$.

If we insert the normal mode solutions (15) in the interface condition (14), we obtain a system of two equations for u_0 and v_0,

$$M(z) \begin{pmatrix} u_0 \\ v_0 \end{pmatrix} = 0,$$

where $M(z)$ is a complex 2×2 matrix. Clearly *the reduced interface problem is GKS-stable if and only if*

$$\det M(z) \neq 0 \quad \text{for } |z| \geq 1$$

In order to check this condition for specific schemes and interface conditions, one needs to have some knowledge of the root structure of the characteristic equations in the critical case $|z| = 1$. The following two lemmas provide this kind of information for dissipative schemes (which we will use in the applications to fluid flows) and also for a wide class of non-dissipative schemes.

LEMMA 1. *Suppose that the subdomain difference schemes* (12) *and* (13) *involve only two time-levels or are identical.*[3] *If these schemes are both dissipative* (*in the sense of Kreiss*), *then for* $|z| = 1$, *the inner roots satisfy*

$$(|\kappa_u| < 1 \text{ and } |\kappa_v| \leq 1) \quad \text{or} \quad (|\kappa_u| \leq 1 \text{ and } |\kappa_v| < 1). \tag{18}$$

Proof. First note that for $|\kappa_u| = 1$, $\kappa_u \neq 1$, we have $|z| < 1$ by assumption that the scheme (12) is dissipative. Thus for $|z| = 1$, either $|\kappa_u| < 1$ or $\kappa_u = 1$. Similarly for $|z| = 1$, either $|\kappa_v| < 1$ or $\kappa_v = 1$. So, it remains to prove that κ_u and κ_v are not both equal to one.

For two time-level schemes, the case $\kappa_u = 1$ or $\kappa_v = 1$ will occur only when $z = 1$ because the schemes are consistent. For $z = 1$, it is well known that 1 is not an inner root for an outflow boundary problem [15, Lemma 5.1]. Thus for $z = 1$, we have either $|\kappa_u| < 1$ or $|\kappa_v| < 1$ because the interface is an outflow boundary either for the left subdomain (if $a > 0$) or the right subdomain (if $a < 0$).

For more than two level schemes, if we had $\kappa_u = \kappa_v = 1$ for some z, then the outer root of (12), which is equal to $1/\kappa_v$ by the assumption that the two schemes are identical, would be equal to the inner root. That is, we would have a multiple root $\kappa_u = 1$ which necessarily occurs when $z = 1$ by the consistency assumption. In this case, the characteristic equation (16) for $z = 1$ would read $(\kappa_u - 1) = 0$ which corresponds to a difference scheme of the following form at steady state ($u_j^{n+1} = u_j^n = u_j$):

$$u_{j+1} - 2u_j + u_{j-1} = 0.$$

Clearly, this is not a consistent approximation of the steady-state part of the exact problem. ∎

[2] Note that if in the left subdomain the cells were numbered from left to right, the outer root would be used in the normal mode solution for u_j^n instead of the inner root.

[3] In fact, due to the particular numbering of the cells in the subdomains, this means that the scheme (12) becomes identical to the scheme (13) when exchanging the subscripts $j + 1$ and $j - 1$.

In order to reveal the importance of the dissipation assumption for schemes (12)–(13), we are going to show that some interface conditions, stable for dissipative schemes, may become unstable for nondissipative schemes. This will be done by considering the class of linear multistep methods (LMM) studied by Beam, Warming, and Yee [3] for initial boundary value problems. The construction of LMM follows the method of lines. It uses a conventional centred difference to approximate the spatial derivative and then a linear multistep method in time for solving the ordinary differential equations. Due to the spatial approximation used, any LMM is nondissipative (at least the Fourier modes corresponding to the wave number $\xi = \pi$ are undamped).

For the present subdomain problem, this class of schemes can be written as

$$\rho(E)u_j^n = \tfrac{1}{2}\eta_u\sigma(E)(u_{j+1}^n - u_{j-1}^n)$$
$$\rho(E)v_j^n = -\tfrac{1}{2}\eta_v\sigma(E)(v_{j+1}^n - v_{j-1}^n),$$

where E is a shift operator in time ($E\phi^n = \phi^{n+1}$), $\rho(E)$ and $\sigma(E)$ denote polynomials in E, and $\eta_u = a\Delta t/\Delta x^{(u)}$, $\eta_v = a\Delta t/\Delta x^{(v)}$. For instance, when $\rho(E) = E - 1$ and $\sigma(E) = E$, we recover the backward Euler scheme.

A LMM is said to be *strongly* A-stable if (see [3]):

(i) it is A-stable, that is, when applied to the linear test equation

$$\frac{du}{dt} = \lambda u, \quad \lambda \in \mathbf{C},$$

its stability region contains all the left half-part of the complex $\lambda\Delta t$ plane and its stability boundary locus is tangent to the imaginary axis only at the origin,

(ii) all roots of $\rho(z) = 0$ are inside the unit circle except for the root $z = 1$.

LEMMA 2. *Assume that the subdomain difference schemes* (12)–(13) *are defined by the same LMM. Then:*

(i) *The two inner roots have opposite signs, that is, for any* z, $\kappa_u = -\kappa_v$;

(ii) *If the LMM is strongly A-stable, then for* $|z| \geq 1$ *and any odd integer* l, *we have the inequality* $z^2 \neq \kappa_u^l\kappa_v^l$.

Proof. (i) The inner roots κ_u and κ_v respectively solve the following characteristic equations:

$$\rho(z) - \tfrac{1}{2}\eta_u\sigma(z)\left(\kappa_u - \frac{1}{\kappa_u}\right) = 0,$$

$$\rho(z) + \tfrac{1}{2}\eta_v\sigma(z)\left(\kappa_v - \frac{1}{\kappa_v}\right) = 0.$$

Thus $\kappa_u = -\kappa_v$.

(ii) Clearly, we have $z^2 \neq \kappa_u^l\kappa_v^l$ for $|z| > 1$ by definition of the inner roots. Now if we had $z^2 = \kappa_u^l\kappa_v^l$, for $|z| = 1$, then from $\kappa_u = -\kappa_v$ we would get $|\kappa_u| = 1$ so that $\frac{1}{2}(\kappa_u - 1/\kappa_u)$ would be purely imaginary. Thus from the characteristic equation, we would have $\mathrm{Re}(\rho(z)/\sigma(z)) = 0$. By assumption that the scheme is A-stable, the stability boundary locus is tangent to the imaginary axis only at the origin and $\mathrm{Re}(\rho(z)/\sigma(z)) = 0$ implies $\rho(z)/\sigma(z) = 0$; hence $\rho(z) = 0$. Furthermore, strong A-stability implies that $\rho(z) = 0$ has only the root $z = 1$ on the unit circle. Consequently, $\kappa_u^l\kappa_v^l = z^2 = 1$ and by $\kappa_u = -\kappa_v$ and the fact that l is odd we would get $\kappa_u^{2l} = -1$. On the other hand, consistency implies $\sigma(1) \neq 0$ so that if we had $\rho(1) = 0$, from the characteristic equation we would obtain $\kappa_u = \pm 1$. This is contradictory, since we could not have both $\kappa_u^{2l} = -1$ and $\kappa_u = \pm 1$. ∎

3. STABLE INTERFACE CONDITIONS FOR ONE-DIMENSIONAL MATCHINGS

We now describe and analyze the stability of interface conditions for some easily workable one-dimensional matchings. Five situations will be considered. The first four have already been described in Section 2.1. They have been named respectively: *continuous matching of first kind* (Fig. 1A), *continuous matching of second kind* (Fig. 1C), *discontinuous matching of first kind* (Fig. 1B), and *discontinuous matching of second kind* (Fig. 1D). The fifth one deals with a regular mesh overlapping.

Conservation of these interface conditions for nonlinear problems will be discussed in Section 4.

3.1 *Continuous Matching of First Kind*

This case often arises when the purpose of domain decomposition is parallel computing. This is the simplest situation for which an accurate interface condition can be easily obtained. The main idea of extending an interface condition to the case of implicit schemes, allowing for stable and uncoupled solution of implicit difference equations in each subdomain, is presented here. A discussion is also presented on the importance of correctly lagging in time the interface values that depend on the adjacent subdomain.

As there is no mesh refinement and the interface is located at the middle of $j = 0$ and $j = 1$ in each subdomain (see Fig. 1A), the boundary cell $j = 0$ in one subdomain coincides exactly with the first interior cell $j = 1$ in the adjacent subdomain.

An obvious time accurate interface condition can be written as

$$u_0^{n+1} = v_1^{n+1}, \quad v_0^{n+1} = u_1^{n+1}. \tag{19}$$

This interface condition has been studied by Ciment [9] for matching different explicit multipoint difference schemes. According to Ciment, for any pair of dissipative difference schemes, the interface problem with this interface condition is

GKS-stable. Unfortunately, the condition (19) does not allow for *uncoupled* multidomain calculation when the difference equations are implicit. We therefore need to lag it in time. The simplest choice is to define the interface condition at the actual time step $n + 1$, using the solutions at the previous time step n. This leads to the following interface condition:

$$u_0^{n+1} = v_1^n, \quad v_0^{n+1} = u_1^n. \tag{20}$$

The interface condition (20) is quite simple to implement and allows for uncoupled and, thus, parallel computations. Another simple interface condition is defined by

$$u_0^{n+1} = v_1^n, \quad v_0^{n+1} = u_1^{n+1}. \tag{21}$$

That is, we first solve the difference equation for u using $u_0^{n+1} = v_1^n$, thus giving the solution u_1^{n+1}; then we define v_0^{n+1} by $v_0^{n+1} = u_1^{n+1}$ and solve the difference equation for v. However, such a condition is not suitable for parallel computing.

More generally, the interface condition can be written as

$$\begin{aligned} u_0^{n+1} &= (1 - \alpha^v)v_1^n + \alpha^v v_1^{n+1}, \quad 0 \le \alpha^v \le 1, \\ v_0^{n+1} &= (1 - \alpha^u)u_1^n + \alpha^u u_1^{n+1}, \quad 0 \le \alpha^u \le 1. \end{aligned} \tag{22}$$

Clearly, this includes the particular interface conditions (19), (20), and (21).

Let us now state the stability results.

PROPOSITION 1. *Assume that the difference schemes* (12)–(13) *involve two time levels or are identical. If these schemes are dissipative, then the reduced problem with interface condition* (22) *is GKS-stable.*

Proof. The determinant of the associated matrix $M(z)$ for the condition (22) is found to be

$$\det M(z) = z^2 - \kappa_u \kappa_v [z\alpha^u + 1 - \alpha^u][z\alpha^v + 1 - \alpha^v].$$

This determinant is different from zero for $|z| > 1$, because $|\kappa_u| < 1$ and $|\kappa_v| < 1$ for $|z| > 1$ and, according to Lemma 1, it is also different from zero in the critical case $|z| = 1$ because of the inequalities (18). Therefore, the problem is stable. ∎

Although dissipation of the difference schemes is sufficient here for the reduced problem to be stable, it is not necessary. To see that, we consider only the interface condition (20).

PROPOSITION 2. *Assume that the difference schemes* (12)–(13) *are defined by the same linear multistep method. If these schemes are strongly A-stable, then the reduced problem with interface condition defined by* (20) *is GKS-stable.*

Proof. Here we have

$$\det M(z) = z^2 - \kappa_u \kappa_v.$$

Using Lemma 2, one can check that $\det M(z) \neq 0$ for $|z| \ge 1$. ∎

In practice, condition (22) is difficult to apply for $0 < \alpha^u \le 1$ and $0 < \alpha^v \le 1$. It requires some iterative method. Here, since we are interested in steady-state flow computations, we will only implement the time-inaccurate condition (20) corresponding to $\alpha^u = 0$ and $\alpha^v = 0$. To enhance the time accuracy of the matching, it may be interesting to define some intermediate condition between (19) and (20) by using a different matching on the right-hand (explicit) and left-hand (implicit) sides of the schemes, that is, by lagging in time the interface values only at the time level $n + 1$ so that the interface condition can be written:

$$\begin{cases} u_0^n = v_1^n, v_0^n = u_1^n & \text{on the RHS} \\ u_0^{n+1} = v_1^n, v_0^{n+1} = u_1^n & \text{on the LHS.} \end{cases} \tag{23}$$

This is easily feasible, but the stability of (23) is not guaranteed. The GKS-stability theory does not apply directly to condition (23) because it does not have the same form at each time level. The original GKS-theory has been developed for boundary conditions which are translatory in time but not necessarily in space (for boundary conditions which are translatory in time and space, scheme-independent stability critera have been developed by Goldberg and Tadmor [15]). We therefore introduce a shift technique to make the condition (23) translatory in time. It consists of combining the interface condition (23) and the specific difference schemes to obtain a condition at the point $j = 1$. In other words, we view the approximation as if the interior schemes were applied from $j \ge 2$ and the interface condition defined at $j = 1$ instead $j = 0$. The equivalent interface condition depends thus on the specific interior schemes and a numerical study of stability using the automatic analysis of Thunë [47] has shown that it is often unstable even for dissipative difference schemes.

Thus, although the interface condition (20) is quite simple, attention needs to be paid to its implementation, since it should not be reduced to the condition (23).

3.2 *Continuous Matching of Second Kind*

This interface configuration has been shown in Fig. 1C. Here we discuss only a nonconservative treatment, which will be applied in Section 8 to demonstrate the importance of conservation. A conservative treatment will be discussed in Section 4.2.

The interface values u_0^{n+1} and v_0^{n+1} are here defined by averaging

$$\begin{aligned} u_0^{n+1} &= (u_1^{n+1} + v_1^*)/2 \\ v_0^{n+1} &= (v_1^{n+1} + u_1^*)/2, \end{aligned} \tag{24}$$

where

$$\begin{aligned} u_1^* &= (1-\alpha^u)u_1^n + \alpha^u u_1^{n+1}, \quad 0 \le \alpha^u \le 1, \\ v_1^* &= (1-\alpha^v)v_1^n + \alpha^v v_1^{n+1}, \quad 0 \le \alpha^v \le 1. \end{aligned} \tag{25}$$

Condition (24) is nonconservative even for $\alpha^u = \alpha^v = 1$.

PROPOSITION 3. *Assume that the difference schemes* (12)–(13) *involve two levels in time or are identical. If these schemes are dissipative, then the reduced problem with the nonconservative interface condition* (24) *is GKS-stable.*

Proof. For condition (24), we have

$$\begin{aligned} \det M(z) = (2-\kappa_u)(2-\kappa_v)z^2 \\ - \kappa_u\kappa_v[z\alpha^u + (1-\alpha^u)][z\alpha^v + (1-\alpha^v)] \end{aligned}$$

which is different from zero for all $|z| \ge 1$, according to Lemma 1. This proves the stability. ▮

We show below that dissipation is not necessary for stability.

PROPOSITION 4. *Assume that the difference schemes* (12)–(13) *are defined by the same linear multistep method. If these schemes are Cauchy stable, then the reduced problem with the nonconservative interface condition* (24) *is GKS-stable.*

Proof. Consider only the case $\alpha^{(u)} = \alpha^{(v)} = 0$. If we assume $\det M(z) = 0$, we will get

$$z = \pm i\kappa_u/\sqrt{(2-\kappa_u)(2+\kappa_u)}$$

as $\kappa_v = -\kappa_u$, according to Lemma 2. Thus $|z| < 1$ for all $|\kappa_u| \le 1$ and the problem is stable. ▮

3.3. *Discontinuous Matching of First Kind*

If the grid continuity across the interface is not imposed, grid construction becomes relatively easier in each subdomain. Thus we now study interface treatment with mesh refinement as shown in Fig. 1B.

The following condition has been discussed by Browning, Kreiss, and Oliger [6], using the explicit leap-frog scheme in each subdomain:

$$\begin{aligned} (u_0^{n+1} + u_1^{n+1})/2 &= (v_0^{n+1} + v_1^{n+1})/2 \\ (u_0^{n+1} - u_1^{n+1})/\Delta x^{(u)} &= (v_1^{n+1} - v_0^{n+1})/\Delta x^{(v)}. \end{aligned} \tag{26}$$

The condition suitable for implicit schemes reads

$$\begin{aligned} (u_0^{n+1} + u_1^*)/2 &= (v_0^{n+1} + v_1^*)/2 \\ (u_0^{n+1} - u_1^*)/\Delta x^u &= -(v_0^{n+1} - v_1^*)/\Delta x^v, \end{aligned} \tag{27}$$

where u_1^* and v_1^* are defined by (25).

In Section 4.2, we will use the Lax–Wendroff scheme to show how to easily make this interface condition conservative for nonlinear problems.

PROPOSITION 5. *Assume that the difference schemes* (12)–(13) *have two levels in time or are identical. If these schemes are dissipative, then the reduced problem with interface condition* (27) *is GKS-stable.*

Proof. Indeed, if we had $\det M(z) = 0$ for some $|z| \ge 1$, we would get

$$XD = -rCY, \tag{28}$$

where $r = \Delta x^{(u)}/\Delta x^{(v)}$ and

$$\begin{aligned} X &= z - [z\alpha^u + (1-\alpha^u)]\kappa_u, \quad Y = z + [z\alpha^u + (1-\alpha^u)]\kappa_u \\ C &= z - [z\alpha^v + (1-\alpha^v)]\kappa_v, \quad D = z + [z\alpha^v + (1-\alpha^v)]\kappa_v. \end{aligned}$$

By Lemma 1, we have either $YD \ne 0$ or $XC \ne 0$ for any z with $|z| \ge 1$. Without loss of generality, we can consider only the case $YD \ne 0$. Then from (28), we deduce

$$X\overline{Y}/|Y|^2 = -rC\overline{D}/|D|^2,$$

where the overbar denotes the complex conjugate. Here the real parts of $X\overline{Y}$ and $C\overline{D}$ are

$$\begin{aligned} \Re(X\overline{Y}) &= |z|^2 - |[z\alpha^u + (1-\alpha^u)]\kappa_u|^2 \\ \Re(C\overline{D}) &= |z|^2 - |[z\alpha^v + (1-\alpha^v)]\kappa_v|^2. \end{aligned}$$

Using Lemma 1 and the condition $0 \le \alpha^u, \alpha^v \le 1$, we obtain

$$\Re(X\overline{Y}) > 0, \quad \Re(C\overline{D}) \ge 0$$

or

$$\Re(X\overline{Y}) \ge 0, \quad \Re(C\overline{D}) > 0.$$

Therefore for $|z| \ge 1$, condition (28) cannot be satisfied; that is, the hypothesis $\det M(z) = 0$ does not hold and the interface problem with the condition (27) is stable. ▮

3.4. *Discontinuous Matching of Second Kind*

Here we extend the second kind continuous matching to the case of mesh refinement (see Fig. 1D). Again a conservative interface condition can be easily constructed and this will be presented in Section 4.2. Here we analyze a nonconservative treatment obtained by using a linear interpolation,

$$\begin{aligned} u_0^{n+1} &= c_u u_1^{n+1} + (1 - c_u) v_1^* \\ v_0^{n+1} &= c_v v_1^{n+1} + (1 - c_v) u_1^*, \end{aligned} \tag{29}$$

with $c_u = 1/(1 + r)$, $c_v = r/(1 + r)$ and u_1^*, v_1^* are defined by (25).

PROPOSITION 6. *Assume that the difference schemes* (12)–(13) *involve two levels in time or are identical. If these schemes are dissipative, then the reduced problem with the interface condition* (29) *is GKS-stable.*

Proof. The determinant of $M(z)$ is

$$\begin{aligned} \det M(z) = z^2(1 + r - \kappa_u)(1 + r^{-1} - \kappa_v) \\ - \kappa_u \kappa_v [z\alpha^u + (1 - \alpha^u)][z\alpha^v + (1 - \alpha^v)]. \end{aligned}$$

As $|(1 + r - \kappa_u)(1 + r^{-1} - \kappa_v)| > 1$ for $|\kappa_u| \le 1$, $|\kappa_v| \le 1$ and $\min(|\kappa_u|, |\kappa_v|) < 1$, thus Lemma 1 implies that $\det M(z) \neq 0$ for $|z| \ge 1$, showing stability. ∎

3.5. *Matching with Grid Overlapping*

When the two subgrids arbitrarily overlap, then some interpolation procedure is needed to construct interface conditions (see, for instance, [5, 7, 17, 39, 44]). It can be easily proved that when the interior difference schemes are dissipative, then an interface condition obtained by any interpolation formula with positive coefficients is stable (for instance, this has been proved in [39] for the explicit Lax–Wendroff scheme). The situation is different for nondissipative schemes. To prove this, consider the case of a regular overlapping so that the interface condition is defined by

$$u_0^{n+1} = v_l^n, \quad v_0^{n+1} = u_l^n, \tag{30}$$

where l is the number of mesh points contained in the overlap.

PROPOSITION 7. *Assume the difference schemes* (12)–(13) *are defined by the same linear multistep method. If this method is strongly A-stable, then the reduced problem with interface condition* (30) *is GKS-stable if l is odd and not GKS-stable if l is even.*

Proof. For the interface condition (30), we get $\det M(z) = z^2 - \kappa_u^l \kappa_v^l$. If l is odd, stability follows easily from Lemma 2. For $z = 1$, we have either $\kappa_u = -\kappa_v = 1$ or $\kappa_u = -\kappa_v = -1$; thus $\det M(z) = 0$ if l is even and the problem is not GKS-stable. ∎

On overlapping grids, the steady state solutions may not be unique; see [53].

4. CONSERVATIVE TREATMENT OF ONE-DIMENSIONAL INTERFACE PROBLEMS

Since we are interested in computing transonic flows with shocks and other discontinuities, it is important to ensure conservation at grid interfaces. In [5], Berger derived a conservation criterion for a general grid interface. Here we apply this criterion to check the conservation of our interface conditions for nonlinear conservation laws. In case of nonconservation, we present another easily workable interface condition for implicit schemes which is conservative and remains stable.

The analysis is based on the nonlinear hyperbolic conservation law,

$$w_t + h(w)_x = 0,$$

approximated by schemes in conservation form,

$$u_j^{n+1} - u_j^n = \sigma^{(u)}(f_{j+1/2} - f_{j-1/2}), \quad j \ge 1, \tag{31}$$

$$v_j^{n+1} - v_j^n = -\sigma^{(v)}(g_{j+1/2} - g_{j-1/2}), \quad j \ge 1, \tag{32}$$

where $\sigma^{(u)} = \Delta t/\Delta x^{(u)}$, $\sigma^{(v)} = \Delta t/\Delta x^{(v)}$, and $f_{j+1/2}$, $g_{j+1/2}$ are consistent approximations of the exact flux function $h(w)$ in the left and right subdomains. Due to the particular numbering of the cells in the left subdomain, the right-hand sides of (31) and (32) have opposite signs. Schemes (31)–(32) are assumed to reduce to (12)–(13) when $h(w) = aw$, a being a constant.

4.1. *Conservation Analysis of Interface Conditions*

Any interface condition discussed in Section 3 can be written in the condensed form

$$\begin{aligned} u_0^{n+1} &= R_u(u_1^{n+1}, u_1^*, v_1^*) \\ v_0^{n+1} &= R_v(v_1^{n+1}, v_1^*, u_1^*), \end{aligned} \tag{33}$$

where u_1^* and v_1^* are defined by (25).

Berger's conservation criterion can be described as follows. In the case of a Cauchy problem without interface, conservation of the difference scheme can be expressed by stating that the following quantity is conserved in time:

$$S^n = \sum_{j=-\infty}^{\infty} \Delta x_j w_j^n. \tag{34}$$

When there is an interface, a similar quantity can be defined

which can be split into three parts accounting for the contributions from the left and right subdomains and the interface:

$$S^n = S^n_{D_u} + S^n_{D_v} + S^n_{\text{interface}}. \tag{35}$$

If $S^{n+1} = S^n$ for any n, the interface treatment is conservative. In this case, if the numerical solution of the interface problem is convergent, it converges to a weak solution of the exact problem; *i.e.*, it allows for a correct shock capturing. For the present problem, the condition $S^{n+1} = S^n$ for any n ensures continuity of the numerical flux at each interface.

In any case, the quantity S^n should be a consistent approximation to the integral $\int_{-\infty}^{\infty} w dx$ of the exact solution w. When approximating this integral by the mid-point formula, we find (in the case of discontinuous matchings, we have assumed $\Delta x^{(u)}/\Delta x^{(v)} = 2$ in order to simplify the notations):

- Continuous matching of first kind ($\Delta x^{(u)} = \Delta x^{(v)} = \Delta x$),

$$\begin{aligned} S^n = &\sum_{j\geq 2}^{\infty} \Delta x u_j^n + \sum_{j\geq 2}^{\infty} \Delta x v_j^n \\ &+ \tfrac{1}{2}\Delta x(u_0^n + v_1^n) + \tfrac{1}{2}\Delta x(v_0^n + u_1^n) \end{aligned} \tag{36}$$

- Discontinuous matching of first kind,

$$\begin{aligned} S^n = &\sum_{j\geq 2}^{\infty} \Delta x^{(u)} u_j^n + \sum_{j\geq 3}^{\infty} \Delta x^{(v)} v_j^n \\ &+ \tfrac{1}{2}\Delta x^{(u)} u_1^n + \tfrac{1}{2}\Delta x^{(u)}[u_0^n + \tfrac{1}{2}(v_1^n + v_2^n)] \\ &+ \tfrac{1}{2}\Delta x^{(v)}(v_0^n + u_1^n) \end{aligned} \tag{37}$$

- Continuous matching of second kind ($\Delta x^{(u)} = \Delta x^{(v)} = \Delta x$),

$$S^n = \sum_{j\geq 1}^{\infty} \Delta x u_j^n + \sum_{j\geq 1}^{\infty} \Delta x v_j^n + \tfrac{1}{2}\Delta x(u_0^n + v_0^n) \tag{38}$$

- Discontinuous matching of second kind,

$$\begin{aligned} S^n = &\sum_{j\geq 1}^{\infty} \Delta x^{(u)} u_j^n + \sum_{j\geq 2}^{\infty} \Delta x^{(v)} v_j^n \\ &+ \tfrac{1}{4}\Delta x^{(u)} u_0^n + \tfrac{1}{2}\Delta x^{(v)}(u_0^n + v_0^n) \\ &+ \tfrac{1}{4}\Delta x^{(v)}(u_0^n + v_1^n). \end{aligned} \tag{39}$$

Introducing the corresponding interface conditions into these quantities and using the schemes (31) and (32) we easily obtain:

PROPOSITION 8. *Assume that in the interface conditions* $\alpha^u = 1$ *and* $\alpha^v = 1$. *Then the interface problem with the interface condition* (22) *is conservative and those with the interface conditions* (24), (27), *and* (29) *are not conservative.*

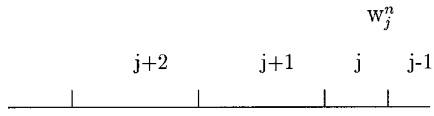

FIG. 2. Nonuniform grid.

4.2. *Conservative Treatment for Various Interface Configurations*

We have just shown that among the first four interface configurations studied in Section 3, only the first interface treatment is conservative. Thus we need to construct a conservative interface condition for the second, third, and fourth interface configurations. The fifth configuration has been studied in detail for explicit schemes in [5] and will not be considered here for implicit schemes.

We first consider the interface condition (27) for the discontinuous matching of the first kind and use the Lax–Wendroff scheme written on a nonuniform grid to show how to easily make this condition conservative without changing its stability property. At the end of this section we will make conservative the continuous and discontinuous matchings of the second kind by transforming them to the first kind.

On a nonuniform grid (shown on Fig. 2), the Lax–Wendroff scheme can be written as

$$w_j^{n+1} - w_j^n = -\sigma_j(h_{j+1/2} - h_{j-1/2}),$$

where the numerical flux $h_{j+1/2}$ is given by

$$\begin{aligned} h_{j+1/2} = &(1 - \theta_j)h(w_j^n) + \theta_j h(w_{j+1}^n) \\ &- \tfrac{1}{2}\sigma_{j+1/2}A(w_{j+1/2}^n)(h(w_{j+1}^n) - h(w_j^n)) \end{aligned}$$

with $\sigma_j = \Delta t/\Delta x_j$, $w_{j+1/2}^n = (1 - \theta_j)w_j^n + \theta_j w_{j+1}^n$, $\sigma_{j+1/2} = (1 - \theta_j)\sigma_j + \theta_j\sigma_{j+1}$, and

$$\theta_j = 1/(1 + r_j), \quad r_j = \Delta x_{j+1}/\Delta x_j.$$

Instead of considering the matching configuration shown in Fig. 1B, we will move each interface cell $j = 0$ to the position of $j = 1$ in the adjacent subdomain so that the interface configuration becomes as shown in Fig. 3, and we apply the interface

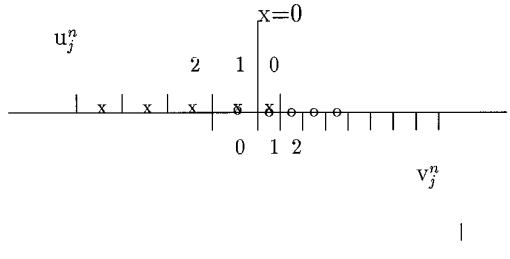

FIG. 3. Discontinuous matching of first kind: nonuniform grid approach.

condition (22) as if there were no mesh refinement. In this way the interface problem is redefined by the schemes in conservative form (31)–(32) with the numerical fluxes,

$$\begin{aligned} f_{j+1/2} &= (1-\theta_j^{(u)})h(u_j^n) + \theta_j^{(u)}h(u_{j+1}^n) \\ &\quad + \tfrac{1}{2}\sigma_{j+1/2}^{(u)}A(u_{j+1/2}^n)(h(u_{j+1}^n) - h(u_j^n)) \\ g_{j+1/2} &= (1-\theta_j^{(v)})h(v_j^n) + \theta_j^{(v)}h(v_{j+1}^n) \\ &\quad - \tfrac{1}{2}\sigma_{j+1/2}^{(v)}A(v_{j+1/2}^n)(h(v_{j+1}^n) - h(v_j^n)), \end{aligned} \tag{40}$$

and the interface condition,

$$\begin{aligned} u_0^{n+1} &= (1-\alpha^v)v_1^n + \alpha^v v_1^{n+1} \\ v_0^{n+1} &= (1-\alpha^u)u_1^n + \alpha^u u_1^{n+1}. \end{aligned} \tag{41}$$

The corresponding quantity S^n reduces to

$$\begin{aligned} S^n &= \sum_{j\geq 2}^{\infty} \Delta x^{(u)} u_j^n + \sum_{j\geq 2}^{\infty} \Delta x^{(v)} v_j^n \\ &\quad + \tfrac{1}{2}\Delta x^{(v)}(u_0^n + v_1^n) + \tfrac{1}{2}\Delta x^{(u)}(v_0^n + v_1^n) \end{aligned}$$

which conserves in time when $\alpha^{(u)} = \alpha^{(v)} = 1$. Thus the interface problem defined by the above nonuniform grid approach in the interior points and the interface condition (41) for the interface of Fig. 3 is conservative at steady state.

Furthermore, it can be easily shown that this interface problem is linearly equivalent to the one defined by the uniform grid approach at the interior points and the interface condition (27) for the interface of Fig. 1B, which has been proved to be linearly stable in Section 3.3. In consequence, we have:

PROPOSITION 9. *The interface problem based on the Lax–Wendroff scheme written on a nonuniform grid* (31), (32), (40) *and the interface condition* (41) *with* $\alpha^u = \alpha^v = 1$ *is conservative and linearly GKS-stable.*

In our applications, we have used an implicit scheme of Lax–Wendroff type. For this scheme we can easily show that Proposition 9 remains valid. For other three-point schemes similar results can be easily obtained.

Let us finally consider the continuous and discontinuous matchings of the second kind. To make them conservative, we transform them into matchings of the first kind by introducing a third mesh near the interface. This mesh involves only one interior point and two interface points (see Fig. 4A for the continuous case and Fig. 4B for the discontinuous case).

In the continuous case, the interface condition is defined by

$$\begin{aligned} u_0^{n+1} &= (1-\alpha^w)w_1^n + \alpha^w w_1^{n+1}, \quad 0 \leq \alpha^w \leq 1, \\ v_0^{n+1} &= (1-\alpha^w)w_1^n + \alpha^w w_1^{n+1}, \quad 0 \leq \alpha^w \leq 1, \end{aligned} \tag{42}$$

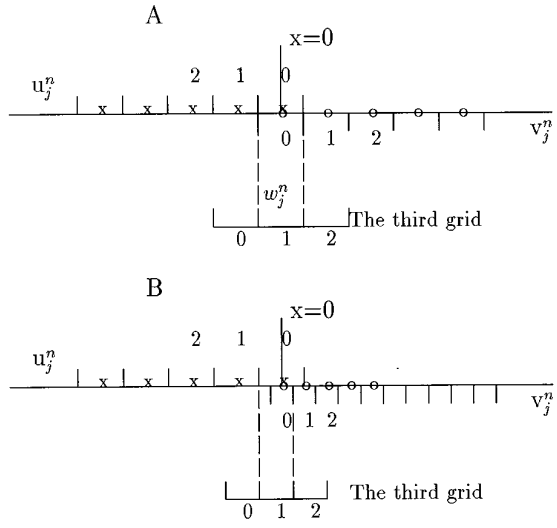

FIG. 4. Transformation of matchings of second kind into matchings of first kind by adding a third grid: (A) continuous matching; (B) discontinuous matching.

where w_1^{n+1} is the solution of another difference equation defined on the third mesh, using the interface conditions

$$\begin{aligned} w_0^{n+1} &= (1-\alpha^u)u_1^n + \alpha^u u_1^{n+1}, \quad 0 \leq \alpha^u \leq 1, \\ w_2^{n+1} &= (1-\alpha^v)v_1^n + \alpha^v v_1^{n+1}, \quad 0 \leq \alpha^v \leq 1. \end{aligned} \tag{43}$$

It can be easily verified that this treatment is conservative if $\alpha^u = \alpha^v = \alpha^w = 1$. This is a two-interface problem, each being (linearly) GKS-stable. However, the stability of each interface does not necessarily ensure the stability of the global problem as shown in [50]. In the present situation, stable behaviour has been observed in all our applications.

The interface condition for the discontinuous case is defined in the following way. As in the continuous case, the matching is reduced to a discontinuous matching of first kind between the left subdomain and the third grid, plus another discontinuous matching of the first kind between the third grid and the right subdomain. For each of these two matchings, we use a nonuniform grid approach as discussed above for the interior schemes and an interface condition similar to (41) so that the approximation is conservative if $\alpha^u = \alpha^v = \alpha^w = 1$.

4.3. *Conservation at Steady State*

Above we discussed the conservation for the time-accurate case $\alpha^u = \alpha^v = 1$. Here we consider the conservation at steady state. An approximation is said to be *conservative at steady state* if it is a convergent solution of a time-dependent conservative treatment or equivalently the numerical flux is continuous across any cell face at steady state.

Clearly, the *steady-state* solutions of the interface problems do not depend on the parameters α^u and α^v. Therefore, the

various matchings will be conservative at steady state for any values of these parameters, provided they are conservative for $\alpha^u = \alpha^v = 1$. So we obtain:

PROPOSITION 10. *Consider the general case* $0 \le \alpha^u \le 1$ *and* $0 \le \alpha^v \le 1$. *Then the continuous matching of first kind with the interface condition* (22), *the discontinous matching of first kind with the condition* (41), *and the matching of second kind with the condition* (42)–(43) *are all conservative at steady state.*

5. STABILITY OF MULTIDIMENSIONAL INTERFACE PROBLEMS

Michelson [31] has extended the one-dimensional GKS-stability theory to multidimensional problems for strictly hyperbolic systems approximated by dissipative schemes. The stability analysis is not as simple as in the one-dimensional case because generally we cannot diagonalize a multidimensional hyperbolic system. To overcome this difficulty, Michelson also proposed a technique to stabilize any multidimensional problem when it is stable in the one-dimensional case. In this section, we first recall briefly how to analyze the stability of a multidimensional interface problem. Then we show that we can get stability results only for particular cases such as a scalar equation. Finally we show how to efficiently extend the stabilizing technique of Michelson to multidomain treatment.

5.1. *Formulation*

As in the one-dimensional case, we assume that all the exterior boundary treatments are stable; thus we only need to consider a Cauchy problem with an interface at $x_1 = 0$, for the hyperbolic system

$$W_t + A_1 W_{x_1} + \sum_{r=2}^{d} A_r W_{x_r} = 0, \tag{44}$$

where $W(x, t) \in \mathbf{R}^m$, $x = (x_1, x_-) \in \mathbf{R}^d$, $x_- = (x_2, ..., x_d)$, $t \in \mathbf{R}^+$, and A_r, $r = 1, ..., d$, are constant $m \times m$ matrices such that A_1 is nonsingular and, for any unit vector $\nu = (\nu_r) \in \mathbf{R}^d$, the matrix $\sum_{r=1}^{d} \nu_r A_r$ has m real eigenvalues and a complete set of eigenvectors. We also assume that all these eigenvalues are distinct; i.e., (44) is strictly hyperbolic.

System (44) is approximated by a difference scheme in the left half-space $x_1 < 0$ and a difference scheme in the right half-space $x_1 > 0$ and some condition is prescribed at the interface $x_1 = 0$. Denote the solutions of the difference equation for $x_1 < 0$ by $U^n_{j_1,j_-}$ and those of the difference equation for $x_1 > 0$ by $V^n_{j_1,j_-}$, where the integer j_1 is relative to x_1 and the multiinteger j_- to x_-.

To analyze the stability, we Fourier-transform the corresponding difference equations with respect to x_- and obtain expressions of the form

$$\sum_{p=-1}^{1} \hat{B}^{(u)}_p \hat{U}^{n+1}_{j_1+p} = \sum_{q=0}^{s} \sum_{p=-1}^{1} \hat{C}^{(u)}_{p,q} \hat{U}^{n-q}_{j_1+p}, \quad j_1 = 1, 2, ..., \tag{45}$$

$$\sum_{p=-1}^{1} \hat{B}^{(v)}_p \hat{V}^{n+1}_{j_1+p} = \sum_{q=0}^{s} \sum_{p=-1}^{1} \hat{C}^{(v)}_{p,q} \hat{V}^{n-q}_{j_1+p}, \quad j_1 = 1, 2, ... \tag{46}$$

The dual variable of x_- will be denoted by ξ_-.

The normal mode solutions of (45) and (46) then take the form

$$\hat{U}^n_{j_1} = z^n \sum_{\nu=1}^{m} \kappa^j_{u_\nu} \Theta_{u_\nu} u_\nu, \quad \hat{V}^n_{j_1} = z^n \sum_{\nu=1}^{m} \kappa^j_{v_\nu} \Theta_{v_\nu} v_\nu, \tag{47}$$

where $\kappa_{u_\nu} = \kappa_{u_\nu}(z, \xi_-)$ and $\kappa_{v_\nu} = \kappa_{v_\nu}(z, \xi_-)$ with $\nu = 1, ..., m$ are the inner roots of the characteristic equations of (45) and (46), Θ_{u_ν} and Θ_{v_ν} with $\nu = 1,2, ..., m$ are linearly independent vector coefficients, and u_ν, v_ν with $\nu = 1,2, ..., m$ are unknowns (scalar) to be determined by the interface conditions. As the schemes involve only three points in each space direction and the system is strictly hyperbolic, all the roots κ_{u_ν}, κ_{v_ν} are distinct.

From Lemma 1, we have the obvious result:

LEMMA 3. *For any pair* $(\kappa_u = \kappa_{u_\nu}, \kappa_v = \kappa_{v_\nu})$ *with* $\nu = 1,2, ..., m$ *and* $|\xi_-| \le \sqrt{d-1}\pi$, *Lemma 1 is valid.*

5.2. *Stability Analysis*

We present a stability analysis only for the continuous matching of first kind. The Fourier transform of the multidimensional interface condition reads:

$$\begin{aligned} \hat{U}^{n+1}_0 &= (1-\alpha^v)\hat{V}^n_1 + \alpha^v \hat{V}^{n+1}_1, \quad 0 \le \alpha^v \le 1, \\ \hat{V}^{n+1}_0 &= (1-\alpha^u)\hat{U}^n_1 + \alpha^u \hat{U}^{n+1}_1, \quad 0 \le \alpha^u \le 1. \end{aligned} \tag{48}$$

Introduction of the general solutions (47) into the condition (48) yields

$$\begin{aligned} z \sum_{\nu=1}^{\nu=m} \Theta_{u_\nu} u_\nu &= (z\alpha^v + (1-\alpha^v)) \sum_{\nu=1}^{\nu=m} \kappa_{v_\nu} \Theta_{v_\nu} v_\nu \\ z \sum_{\nu=1}^{\nu=m} \Theta_{v_\nu} v_\nu &= (z\alpha^u + (1-\alpha^u)) \sum_{\nu=1}^{\nu=m} \kappa_{u_\nu} \Theta_{u_\nu} u_\nu \end{aligned}$$

which can be rewritten as

$$M(z)(u_1, ..., u_m, v_1, ..., v_m)^t = 0$$

with the partitioned matrix:

$$M(z) = \begin{bmatrix} F_u & G_v \\ G_u & F_v \end{bmatrix}.$$

The block-elements of the matrix $M(z)$ are defined by $F_u = z\Theta_u$, $F_v = z\Theta_v$,

$$G_u = (z\alpha^u + 1 - \alpha^u)\Theta_u\Lambda_u, \quad G_v = (z\alpha^v + 1 - \alpha^v)\Theta_v\Lambda_v,$$

where $\Theta_u = (\Theta_{u_1}, \Theta_{u_2}, ..., \Theta_{u_m})$, $\Theta_v = (\Theta_{v_1}, \Theta_{v_2}, ..., \Theta_{v_m})$, Λ_u, Λ_v are diagonal matrices with diagonal elements: $\lambda_{u_\nu} = \kappa_{u_\nu}$, $\nu = 1, 2, ..., m$, $\lambda_{v_\nu} = \kappa_{v_\nu}$, $\nu = 1, 2, ..., m$. The matrices F_u and G_v are nonsingular since the fundamental solutions are linearly independent.

Clearly, the determinant of $M(z)$ will not vanish if the same holds for the matrix:

$$M'(z) = M(z)\begin{bmatrix} F_u^{-1} & -F_u^{-1}G_vF_v^{-1} \\ 0 & F_v^{-1} \end{bmatrix} = \begin{bmatrix} I & 0 \\ G_uF_u^{-1} & I - G_uF_u^{-1}G_vF_v^{-1} \end{bmatrix}.$$

Now we have $\det M' = \det(I - G_uF_u^{-1}G_vF_v^{-1})$. *If* $\Theta_u = \Theta_v$, which, occurs, for instance, when $m = 1$ or when all the Jacobian matrices A_i, $i = 1, 2, ..., d$ commute, then

$$\det M' = \det(I - z^{-2}\Lambda_u\Lambda_v), \quad z \neq 0.$$

Using Lemma 3, we find that $\det M'(z) \neq 0$ for all $|z| \geq 1$ and all $|\xi_-| \leq \sqrt{d-1}\pi$; that is, the multidimensional problem is stable.

If $\Theta_u \neq \Theta_v$, we cannot get any conclusion for the stability.

5.3. *A Universal Stabilizing Technique*

In general we do not know whether a problem, stable in the one-dimensional case, remains stable in the multidimensional case. We could examine the eigenvalue problem numerically as done by Thunë [47] for initial boundary value problems without internal interface. Here, we shall rather rediscuss the universal stabilizing technique of Michelson [31] to maintain the stability of a multidimensional interface problem when it is stable in the one-dimensional case, that is when it is stable for $\xi_- = 0$. Michelson proposed this technique originally for multidimensional problem without interface. In the present interface problem, it consists of adding a numerical dissipation in the tangent direction for both the difference schemes and the interface conditions. That is, in the difference schemes, $U^n_{j_1,j_-}$ and $V^n_{j_1,j_-}$ are replaced by

$$(I - K\omega(x)\Delta^k_{j_-})U^n_{j_1,j_-}, \quad (I - K\omega(x)\Delta^k_{j_-})V^n_{j_1,j_-},$$

and in the interface conditions, $U^n_{j_1,j_-}$ and $V^n_{j_1,j_-}$ are replaced by

$$(I - K\Delta^k_{j_-})U^n_{j_1,j_-} \quad \text{and} \quad (I - K\Delta^k_{j_-})V^n_{j_1,j_-}.$$

Here K is a scalar constant, k is a positive integer such that $2k$ be equal to or slightly greater than the order of accuracy of the difference schemes in order to maintain the global accuracy of the interface approximation, $\omega(x)$ is a cutoff function which is equal to one near the interface $x = 0$ and decreases to zero apart from it, and Δ_{j_-} is a discrete Laplacian operator on $\mathbf{R}^{d-1}$ defined by

$$\Delta_{j_-} = \sum_{r=2}^{d}(E_r + E_r^{-1} - 2) \quad E_r\phi_{j_1,...,j_r,...,j_d} = \phi_{j_1,...,j_r+1,...,j_d}.$$

Michelson proved that if the one-dimensional problem is stable, then for any k there is always a constant K_0 such that the multidimensional problem is stable for $K > K_0$.

Here we show that for particular interface conditions, the stabilizing technique can be simplified. Suppose that the interface condition without dissipation can be written as

$$\begin{aligned} D_{uu}U^{n+1}_{0,j_-} &= D_{uv}V^{n+1}_{1,j_-}. \\ D_{vv}V^{n+1}_{0,j_-} &= D_{vu}U^{n+1}_{1,j_-}. \end{aligned} \tag{49}$$

Then the interface condition with dissipation is

$$\begin{aligned} D_{uu}U^{n+1}_{0,j_-} - K\Delta^k_{j_-}U^{n+1}_{0,j_-} &= D_{uv}V^{n+1}_{1,j_-} \\ D_{vv}V^{n+1}_{0,j_-} - K\Delta^k_{j_-}V^{n+1}_{0,j_-} &= D_{vu}U^{n+1}_{1,j_-}. \end{aligned} \tag{50}$$

The corresponding matrix $M(z)$ is given by

$$M(z) = \begin{bmatrix} \eta A_u & B_v \\ B_u & \eta A_v \end{bmatrix},$$

where $\eta = 1 + K2^k\sum_{i=2}^{d}(1 - \cos\xi_i)^k$. For convenience, we denote $Q(z, \xi_-) = B_uA_u^{-1}B_vA_v^{-1}$.

PROPOSITION 11. *Suppose that no dissipation is added in the interior difference schemes and the problem with interface condition* (49) *is stable for* $\xi_- = 0$. *If* $\rho(Q(z, 0)) \leq 1$ *for* $|z| \geq 1$, *then there exists a constant* $K > 0$ *such that the problem with interface condition* (50) *is stable for* $|\xi_-| \leq \sqrt{d-1}\pi$.

Proof. The determinant $\det M(z, \xi_-)$ is nonzero if and only if

$$\det(\eta^2 I - Q) \neq 0.$$

As $\rho(Q(z, 0)) \leq 1$ for all $|z| \geq 1$, we can choose K large enough to have

$$\eta^2 > \rho(Q) \quad \forall|\xi_-| \leq \sqrt{d-1}\pi, \ \xi_- \neq 0,$$

so that $\det(\eta^2 I - Q) \neq 0$ and thus $\det M \neq 0$ for all $|z| \geq 1$ and all $|\xi_-| < \sqrt{d-1}\pi$.

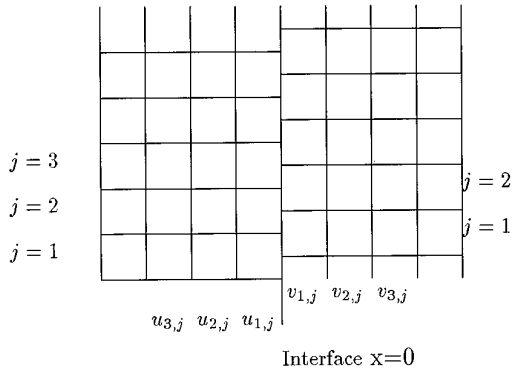

FIG. 5. Patched grid without mesh refinement.

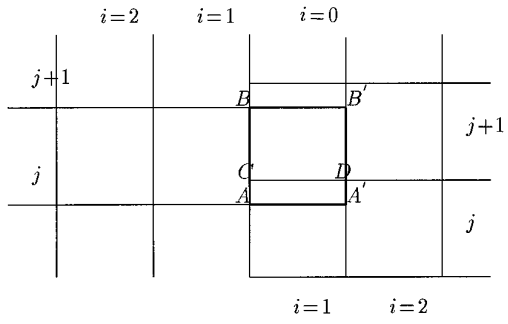

FIG. 6. Patched grid. The interface cell $(0, j)$ of the left subdomain is formed by the corners A, A', B', and B. This cell is divided into two parts by the cell-side line CD of the right subdomain.

For continuous matchings of the first and second kinds, the condition $\rho(Q(z, 0)) \leq 1$ is satisfied for all $|z| \geq 1$; thus *without modifying the interior difference schemes we can ensure stability by using the interface condition* (50).

In our subsequent applications, we have never found a multidimensional instability; thus the stabilizing technique has not been used.

6. A CONSERVATIVE INTERFACE TREATMENT FOR 2D PATCHED GRIDS

In the so-called patched grids, like the one shown in Fig. 5, the two subdomains share a common grid line at the interface but there is no grid continuity across the interface. The use of patched grids makes the construction of the mesh of geometrically complex problems a relatively easy task. The key point with these grids is to define stable and conservative interface conditions.

Rai [42] devised a one-sided flux interpolation method to ensure conservation for a patched grid having a common *cell-center line* at the interface. The interface condition for one subdomain is defined from the conservative variables while for the adjacent subdomain the interface condition is defined from the numerical flux. This can be considered as a particular case of the flux interpolation method of Berger [5]. However, we are not able to obtain general stability results for Rai's method. Here we present a different interface condition which is conservative and unconditionally stable for dissipative difference schemes. Instead of having a common cell-center line, our patched grid technique has a common *cell-side line*. In the one-dimensional case, this is the matching of first kind (Fig. 1A). We will discuss the interface treatment only for the case without mesh refinement. When there is a mesh refinement in the direction normal to the interface, we write the difference schemes on a nonuniform grid (as explained in Section 4.2) to make the interface treatment conservative. The case of mesh refinement in the tangent direction can be included in a direct way.

The present treatment consists in computing the numerical flux for each interface divided segment and summing them to get the total numerical flux for each cell face at the interface. It does not involve any flux interpolation. Furthermore, it is done in such a way that the interface condition is linearly equivalent to the one obtained by area-weighted interpolation and thus is linearly stable.

Let us detail the interface condition for a two-dimensional grid patching. For each subdomain, there is a line of boundary cells located in the adjacent subdomain. Consider the boundary cell of the left subdomain defined by the indexes $i = 0$ and j (see Fig. 6). The corners of this cell are denoted by A, A', B' and B. The cell face AB lying at the interface $x = 0$ is divided into parts AC and CB by the line CD which separates the cells $(1, j)$ and $(1, j + 1)$ of the right subdomain.

Suppose that the x-direction numerical flux at any interior face $(i + \frac{1}{2}, j)$ is of the form

$$f_{i+1/2,j} = \sum_{\sigma=-1}^{s} \theta_\sigma^{(u)} f_\sigma(u_{i,j}^{n-\sigma}, u_{i+1,j}^{n-\sigma}),$$

where the $\theta_\sigma^{(u)}$ denote constant coefficients. Then the numerical flux on the line AB for the left subdomain is computed as:

$$f_{1/2,j} = f_{AC} + f_{CB} \tag{51}$$

$$f_{AC} = \alpha_j \sum_{\sigma=-1}^{s} \theta_\sigma^{(u)} f_\sigma(u_{i,j}^{n-\sigma}, v_{i,j}^{n-\sigma-1}) \tag{52}$$

$$f_{CB} = (1 - \alpha_j) \sum_{\sigma=-1}^{s} \theta_\sigma^{(u)} f_\sigma(u_{1,j}^{n-\sigma}, v_{1,j+1}^{n-\sigma-1}), \tag{53}$$

where $\alpha_j = |\vec{AC}|/|\vec{AB}|$.

For the right subdomain, if the x-direction numerical flux at any interior face $(i + \frac{1}{2}, j)$ is

$$g_{i+1/2,j} = \sum_{\sigma=-1}^{s} \theta_\sigma^{(v)} g_\sigma(v_{i,j}^{n-\sigma}, v_{i+1,j}^{n-\sigma})$$

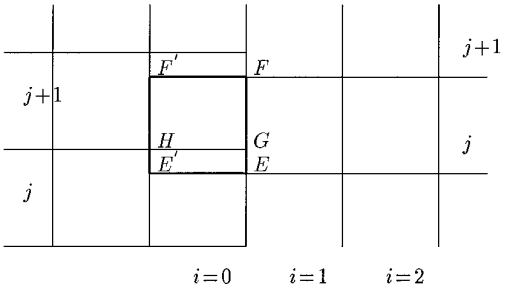

FIG. 7. Patched grid. The interface cell $(0, j)$ of the right subdomain is formed by the corners E, E', F′, and F. This cell is divided into two parts by the cell-side line HG of the left subdomain.

then the numerical flux on the line EF (Fig. 7) is computed by

$$g_{1/2,j} = g_{EG} + g_{GF} \tag{54}$$

$$g_{EG} = \beta_j \sum_{\sigma=-1}^{s} \theta_\sigma^{(v)} g_\sigma(v_{1,j}^{n-\sigma}, u_{1,j}^{n-\sigma-1}) \tag{55}$$

$$g_{GF} = (1-\beta_j) \sum_{\sigma=-1}^{s} \theta_\sigma^{(v)} g_\sigma(v_{1,j}^{n-\sigma}, u_{1,j+1}^{n-\sigma-1}), \tag{56}$$

where $\beta_j = |\vec{EG}|/|\vec{EF}|$.

PROPOSITION 12. *The problem defined by any pair of conservative three-point* (*in each space direction*) *difference schemes and the interface condition* (51)–(56) *is conservative at steady state. Furthermore, it is linearly GKS-stable for any pair of scalar three-point dissipative difference schemes which involve two time levels or are identical.*

Proof. Conservation is obvious. Stability follows from the fact that this interface condition is linearly equivalent to

$$u_{0,j}^n = \alpha v_{1,j}^{n-1} + (1-\alpha) v_{1,j+1}^{n-1}$$
$$v_{0,j}^n = \beta u_{1,j}^{n-1} + (1-\beta) u_{1,j+1}^{n-1}$$

for which the determinant

$$\det M(z, \xi_-) = z^2 - [\alpha + (1-\alpha)e^{i\xi_-}][\beta + (1-\beta)e^{i\xi_-}]\kappa_u \kappa_v$$

is nonzero for $|z| \geq 1$ and $|\xi_-| \leq \pi$. ∎

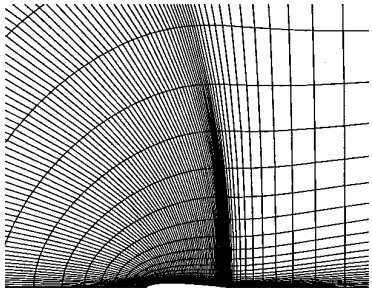

FIG. 8. A 95 × 25 grid for the upper half part of the NACA 0012 airfoil (partial view).

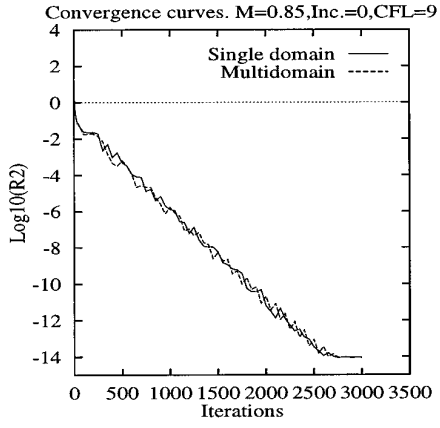

FIG. 9. Convergence histories for single domain and multidomain computations. $M_\infty = 0.85$ and CFL = 9. R is the l_2-residual on the density equation.

The above interface condition has been formulated on a Cartesian mesh but its extension to a curvilinear mesh is straightforward.

7. APPLICATIONS

We present here multidomain calculations of external flows over the NACA 0012 airfoil and a two-element airfoil using the compressible Euler equations. These test cases have been chosen for their sensitivity to the accuracy of the numerical treatments.

7.1. *Implicit Euler Solver*

Present calculations are based on the two-dimensional Euler equations

$$w_t + f(w)_x + g(w)_y = 0 \tag{57}$$

with

$$w = \begin{pmatrix} \rho \\ \rho u \\ \rho v \\ \rho E \end{pmatrix}$$

$$f(w) = \begin{pmatrix} \rho u \\ \rho u^2 + p \\ \rho uv \\ (\rho E + p)u \end{pmatrix}, \quad g(w) = \begin{pmatrix} \rho v \\ \rho vu \\ \rho v^2 + p \\ (\rho E + p)v \end{pmatrix}$$

and, assuming a perfect gas law,

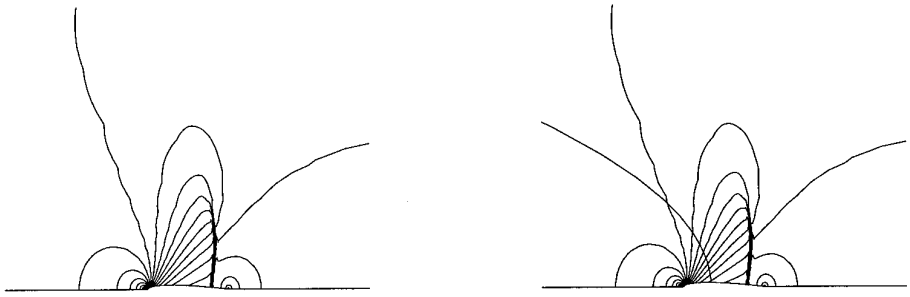

FIG. 10. Pressure contours for $M_\infty = 0.85$, CFL = 9: Left, single domain; Right, multidomain (continuous matching of the first kind).

$$p = (\gamma - 1)\rho[E - \tfrac{1}{2}(u^2 + v^2)],$$

where ρ, p, u, v, and E denote the density, the pressure, the velocity Cartesian components, and the total energy and $\gamma = 1.4$ is the specific heat ratio.

System (57) is approximated by the following implicit centred scheme of second-order accuracy [28], which is a factored implicit version of a Lax–Wendroff-type approximation,

$$\Delta\tilde{w}_{i+1/2,j} = -\Delta t(\delta_1 f/\Delta x + \mu_1\mu_2\delta_2 g/\Delta y)^n_{i+1/2,j}$$

$$\tilde{f}_{i+1/2,j} = [(\mu_1 f)^n + \tfrac{1}{2}(\mu_1 A)^n\,\Delta\tilde{w}]_{i+1/2,j}$$

$$\Delta\tilde{\tilde{w}}_{i,j+1/2} = -\Delta t(\mu_1\mu_2\delta_1 f/\Delta x + \delta_2 g/\Delta y)^n_{i,j+1/2}$$

$$\tilde{\tilde{g}}_{i,j+1/2} = [(\mu_2 g)^n + \tfrac{1}{2}(\mu_2 B)^n\,\Delta\tilde{\tilde{w}}]_{i,j+1/2}$$

$$\Delta w^{\text{expl}}_{i,j} = -\Delta t(\delta_1\tilde{f}/\Delta x + \delta_2\tilde{\tilde{g}}/\Delta y)_{i,j}$$

$$\Delta w^*_{i,j} - \tfrac{1}{2}(\Delta t/\Delta x)^2\delta_1[(\mu_1 A^n)^2\delta_1(\Delta w^*)]_{i,j} = \Delta w^{\text{expl}}_{i,j}$$

$$\Delta w_{i,j} - \tfrac{1}{2}(\Delta t/\Delta y)^2\delta_2[(\mu_2 B^n)^2\delta_2(\Delta w)]_{i,j} = \Delta w^*_{i,j}$$

$$w^{n+1}_{i,j} = w^n_{i,j} + \Delta w_{i,j},$$

where $A = df(w)/dw$ and $B = dg(w)/dw$ are the Jacobian matrices, δ_s, μ_s for $s = 1, 2$ are spatial operators such that for $\phi_{i,j}$ defined at the mesh point $x = i\,\Delta x$ and $y = j\,\Delta y$,

$$(\delta_1\phi)_{i,j} = \phi_{i+1/2,j} - \phi_{i-1/2,j}$$

$$(\delta_2\phi)_{i,j} = \phi_{i,j+1/2} - \phi_{i,j-1/2}$$

$$(\mu_1\phi)_{i,j} = \tfrac{1}{2}(\phi_{i+1/2,j} + \phi_{i-1/2,j})$$

$$(\mu_2\phi)_{i,j} = \tfrac{1}{2}(\phi_{i,j+1/2} + \phi_{i,j-1/2}).$$

If the matrices A and B commute, the above scheme is always linearly stable in L_2 and dissipative, except when A or B is singular. It involves 3×3 points at level n and leads to the solution of block-tridiagonal linear systems. For the Euler equations, for which A and B do not commute, this scheme has a large stability domain. It is always stable for Mach numbers lower than 0.8 or greater than 2.4 and conditionally stable in between with a stability limit depending on the fluid velocity direction. This stability constraint is due to the ADI factorization of the implicit treatment and can be removed by using a line-relaxation technique. See [11, 24] for details.

The above scheme has been implemented on a structured mesh by using a multidomain finite-volume formulation. On a rigid wall, the slip condition is prescribed and the pressure is obtained from a linear combination of the discrete form of the x and y-momentum equations to obtain a conservative approximation of the normal momentum equation. On an external boundary, we prescribe the freestream direction and the entropy and enthalpy for a subsonic inflow, or the pressure for a subsonic outflow. Due to its own dissipative properties, this scheme is used without artificial viscosity as in [28].

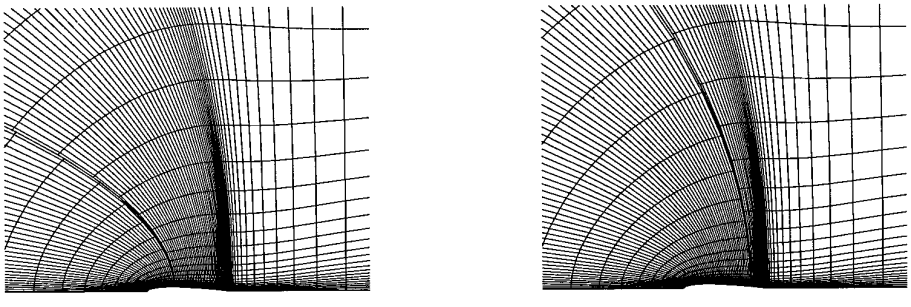

FIG. 11. Patched grids for the upper half part of the NACA 0012 airfoil (partial view): Left, first interface position; Right, second interface position.

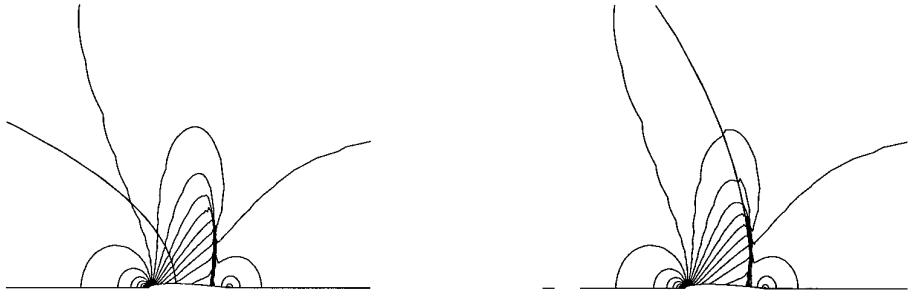

FIG. 12. Pressure contours ($\Delta p = 0.05$) for $M_\infty = 0.85$, CFL = 9, computed using patched grids: Left, first interface position (located in the supersonic region); Right, second interface position (aligned with the shock).

7.2. *Comparison between Multidomain and Single Domain Calculations*

To make a direct comparison between single domain and multidomain computations, we first calculate the flow over the upper half of the NACA 0012 airfoil at zero angle of attack, using symmetry boundary conditions on the symmetry line. The mesh for the single domain computation is displayed in Fig. 8. Continuous grids and patched grids will be considered.

We first compute the flow at Mach number $M_\infty = 0.85$ using two subdomains with grid continuity; that is, the mesh is cut at some vertical mesh line to form two subdomains for multidomain calculations. The interface crosses the supersonic pocket (see Fig. 10). We apply here *the continuous matching of the first kind* with the interface condition (20). The convergence histories for the single- and two-domain computations using the same CFL number (CFL = 9) are shown in Fig. 9. We see the multidomain calculation converges as well as the single domain calculation although the interface condition has been lagged in time.

We then compute the same flow using patched grids. Two interface positions are tested. In the first one the interface crosses the supersonic pocket and in the second one it is partially aligned with the shock. The corresponding patched grids are shown in Fig. 11. The pressure contours for both of the interface positions are displayed in Fig. 12.

Comparison of the convergence histories for single and bidomain calculations with patched grids is presented in Fig. 13. When the interface crosses the supersonic flow region, the convergence of the patched grid technique is only slightly delayed, in comparison with the single domain computation. When the interface is aligned with the shock, the number of time iterations required to reach the zero-machine convergence is increased by 15% with respect to the single domain calculation. From the pressure contours we see that there is very little difference between the single domain solution and the multidomain solutions with patched grids. As the grid is highly discontinous across the interface in patched grid computation, we cannot expect perfect continuity of pressure contours, even though the interface condition is quite accurate, because in our graphic code we have an interpolation different from the one used in the interface conditions.

7.3. *Various Multidomain Computations of a Transonic Flow over a NACA0012 Airfoil*

We now compute a transonic flow at Mach number $M_\infty = 0.85$ and angle of attack $\alpha = 1°$ over the NACA 0012 airfoil using different multidomain techniques. In each case, we have used CFL = 9.

The first technique is based on the C-mesh shown in Fig. 14. The airfoil is represented by a cell-center line. The two ends of this line join at the trailing edge to form a double-defined line (Fig. 15A) which is considered as an interface. Thus, we define a single domain computation, where one part of the domain is matched to another part of the same domain. Clearly, the matching at the interface is continuous of the second kind. A simple averaging is applied at the interface, that is, the *nonconservative interface condition* (24) with $\alpha^u = \alpha^v = 0$. In the second technique used here, the original C-mesh is cut on the two vertical mesh lines passing through the trailing edge

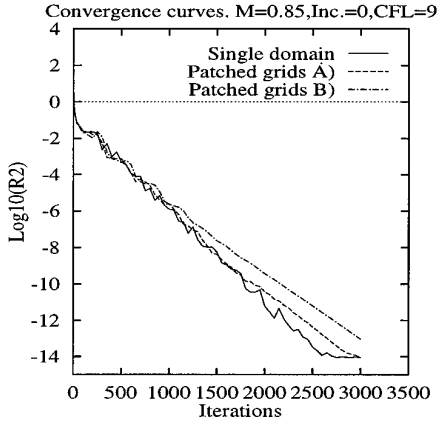

FIG. 13. Convergence histories for single domain and patched grid multidomain computations. $M_\infty = 0.85$, CFL = 9.

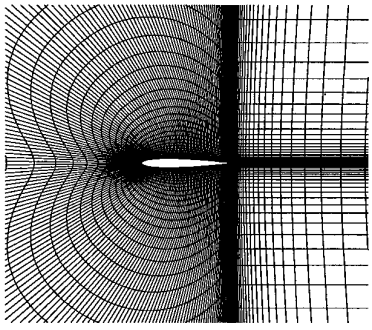

FIG. 14. C-mesh with 257 × 33 points (partial view).

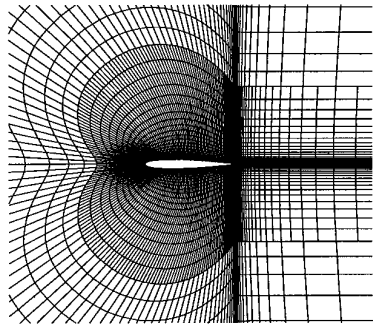

FIG. 16. Patched grid with mesh refinement (8084 points).

to form two subdomains: one upstream of the trailing edge and the other downstream (Fig. 15B). The continuous matching of the first kind with the interface condition (20) is applied. In the third technique, the domain is divided into three parts (Fig. 15C): the near field upstream of the trailing edge equipped with the same mesh as previously, its continuation downstream of the trailing edge, and the far field using a coarse C-mesh matched without continuity. The composite grid is shown in Fig. 16.

The convergence histories for the three techniques are shown in Fig. 17. The convergence histories are quite different for the three techniques. Surprisingly, the third technique, which uses the most subdomains, has the best convergence rate. The first technique, which has a single domain and which uses a nonconservative interface condition, converges more slowly than the other two. To reach a residual of $R = 10^{-5}$, the number of time iterations of the one-domain technique is two times that of the tridomain technique. The reason seems to be that the outside subdomain has a coarse grid, which annihilates some waves dominating the influence on the convergence rate. Thus, increasing the number of subdomains does not necessarily delay the convergence rate.

The pressure contours with different matching techniques are shown in Fig. 18. The pressure distributions on the walls are displayed in Fig. 19. We see that the third technique, which involves mesh refinement, produces some oscillations near the interface at the refined side. It is well known that mesh refinement could induce oscillations. One example has been shown in [6]. As has been pointed out by Kreiss [27], oscillations near a boundary can be eliminated by adding some tangent dissipation. Despite the oscillations, the third technique is always stable and gives a correct shock position (Fig. 19) which depends strongly on the conservation of the numerical approximation. The one-domain technique, which uses a nonconserva-

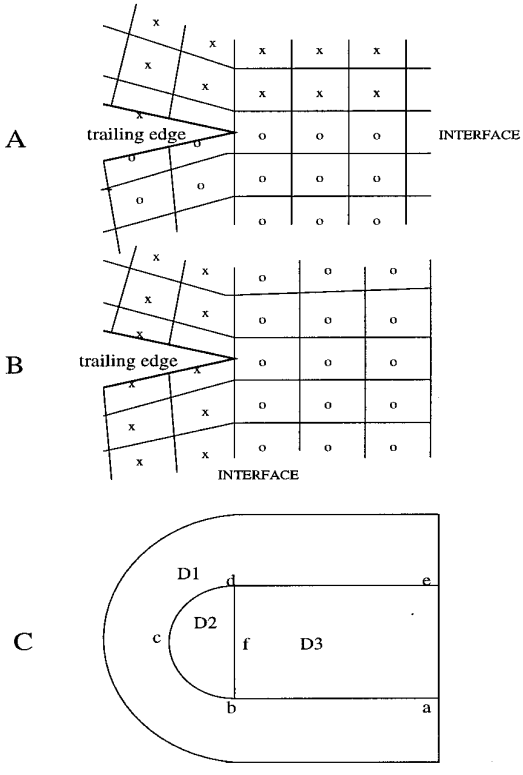

FIG. 15. Subdomain distributions: (A) One-domain treatment (continuous matching of second kind); (B) Bidomain treatment (continuous matching of first kind); (C) Tridomain treatment (continuous matching at line *bfd* and discontinuous matching at line *abcde*; see Fig. 16).

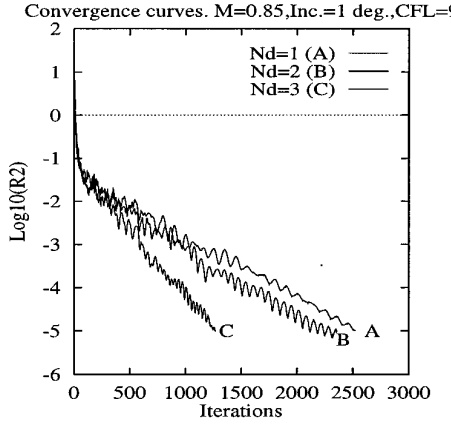

FIG. 17. Convergence histories for three different multidomain treatments. $M_\infty = 0.85$, $\alpha = 1°$, CFL = 9.

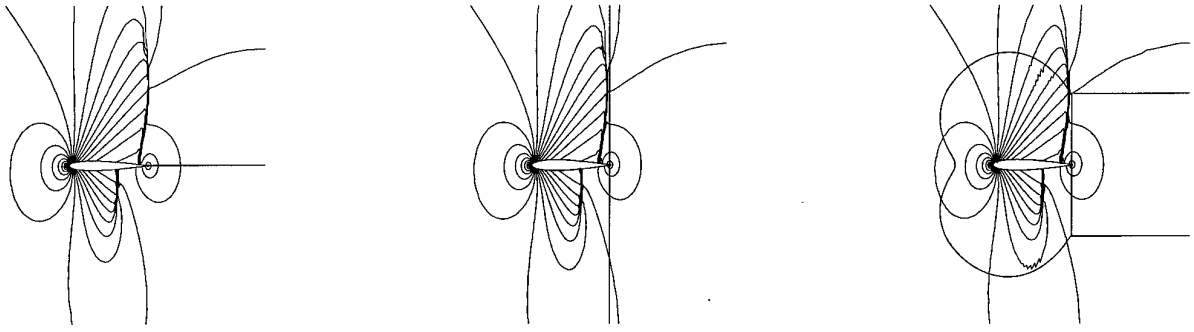

FIG. 18. Pressures contours ($\Delta p = 0.05$) with $M_\infty = 0.85$, $\alpha = 1°$, CFL = 9: Left, one domain (non-conservative); Middle, two subdomains (conservative); Right, three subdomains (conservative).

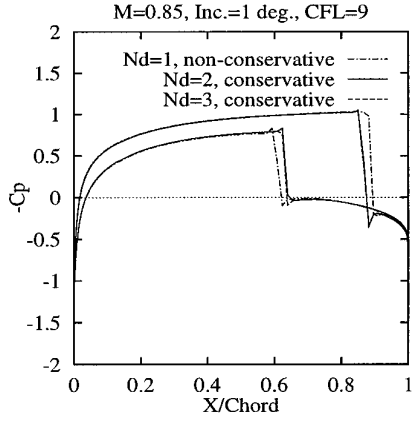

FIG. 19. Pressure distributions on the airfoil for three different multidomain treatments. $M_\infty = 0.85$, $\alpha = 1°$, CFL = 9.

tive interface condition, gives a wrong shock position. It leads to a lift coefficient $C_l = 0.424$ which is much greater than the expected and more accurate value $C_l = 0.376$ reported in [28] for a very fine grid. The bidomain technique yields $C_l = 0.366$ and the tridomain technique leads to $C_l = 0.370$.

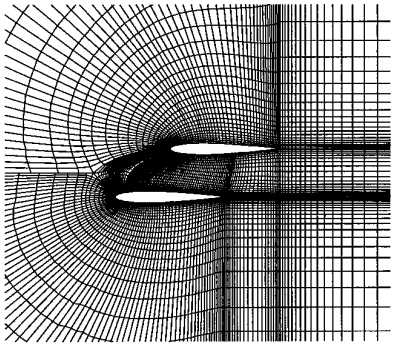

FIG. 20. Patched grid for the two-element airfoil (partial view). Five subdomains and 8340 cells.

7.4. *Flow over a Two-Element Airfoil*

Finally, we compute a transsonic flow around a two-element airfoil formed by two parallel NACA0012 airfoils. They are shifted by a distance equal to a half chord in both the parallel and perpendicular directions. The free-stream Mach number $M_\infty = 0.7$ and there is no angle of attack. Previous computations have been done either on a Cartesian grid [10, 33] or an unstructured grid [20]. To the authors' knowledge, there is no other computation of this test case based on curvilinear meshes.

The composite grid we use is displayed in Fig. 20. It is made up of five subdomains. One subdomain is located above the upper airfoil, another is beneath the lower airfoil, two others are between the airfoils and the final one is downstream of the trailing edge of the upper airfoil. The total number of cells is 8340. The flow has been computed using our conservative interface condition for patched grids. The convergence history for CFL = 8 is shown in Fig. 21. The convergence is quite regular and rapid for this type of problem. Only 1000 iterations are needed to reach a l_2 residual on the density equation of 10^{-5}. The pressure distribution around the airfoils is shown in Fig. 22. Figure 23 presents a comparison of the pressure con-

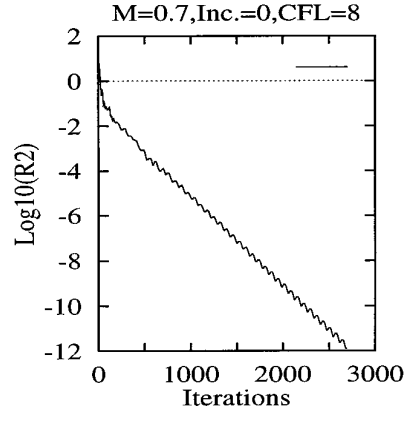

FIG. 21. Convergence history for the two-element airfoil. $M_\infty = 0.7$, CFL = 8.

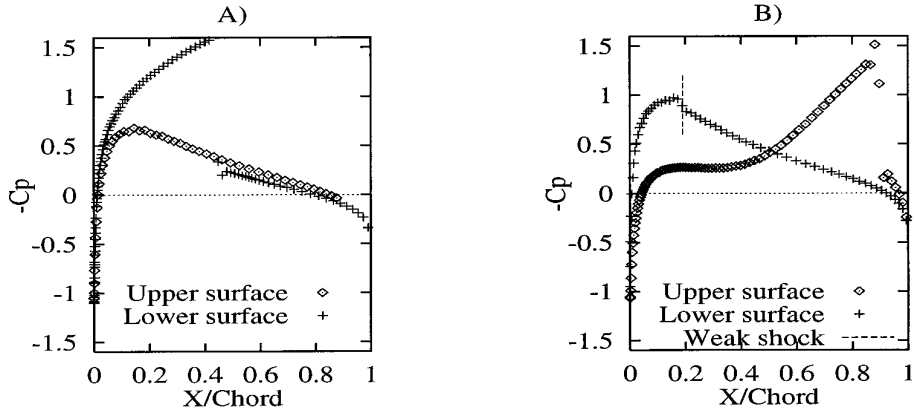

FIG. 22. Pressure distribution along the airfoils. $M_\infty = 0.7$, CFL = 8: (A) C_p along the upper airfoil; (B) C_p along the lower airfoil (location of the weak shock, dashed line).

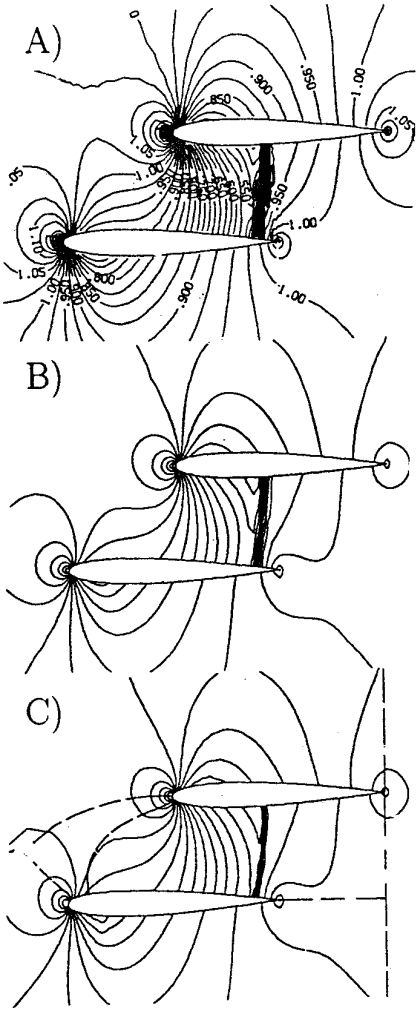

FIG. 23. Pressure contours: (A) Cartesian grid method of Clarke, Salas, and Hassan ($\Delta p = 0.025$, mesh point number not mentioned); (B) cartesian grid method of Morinishi ($\Delta p = 0.05$, 7743 mesh points); (C) present multidomain method ($\Delta p = 0.05$, 8340 mesh points).

tours obtained by the present multidomain technique and those of [10, 33], where centred Runge–Kutta methods are used on Cartesian grids. The three flow fields are quite similar. Notably, a strong shock wave exists between the two airfoils. However, there are two new features in the present results. First, the strong shock is better resolved. Second, a weak shock appears on the lower surface of the lower airfoil, as can be seen from the pressure distribution (Fig. 22). Let us also note that the quality of the results obtained in [20] with a method using an unstructured grid is poor with respect to the methods using Cartesian or patched curvilinear grids.

8. CONCLUDING REMARKS

Interface conditions which are conservative, GKS-stable and ensure convergence to a steady state have been proposed for computing compressible steady flows using implicit finite difference schemes on multiblock grids. The present multidomain method deals with the cases of continuous as well as patched grids with and without mesh refinement. Since it leads to independent solutions of implicit difference schemes in each subdomain, it can be easily implemented on parallel computers. Typical numerical results have been obtained for transonic flows over single- and two-element airfoils. The comparison between single domain and multidomain computations shows that domain decomposition does not necessarily delay the convergence to steady state because it allows for a more efficient grid distribution. The comparison with the results obtained by accurate Cartesian grid methods for the two-element airfoil demonstrates the accuracy of the present multidomain method.

ACKNOWLEDGMENTS

This work was supported by DRET (French Ministry of Defence) under Contracts 90/162 and 92/169. The authors are grateful to Professor E. Tadmor (Tel-Aviv University) for suggesting the shift technique discussed at the end of Section 3.1 and to Doctor M. Thuné (Uppsala University) for kindly providing us with his IBstab II code for numerically checking GKS-stability of a general initial-boundary value problem.

REFERENCES

1. F. Angrand and A. Dervieux, *Int. J. Numer. Methods Fluids* **4,** 749 (1984).
2. O. Baysal, K. Fouladi, and V. R. Lessard, *AIAA J.* **29,** 903 (1991).
3. R. M. Beam, R. F. Warming, and H. C. Yee, *J. Comput. Phys.* **48,** 200 (1982).
4. M. J. Berger, *Math. Comput.* **45,** 301 (1985).
5. M. J. Berger, *SIAM J. Numer. Anal.* **24,** 967 (1987).
6. G. Browning, H.-O. Kreiss, and J. Oliger, *Math. Comput.* **27,** 29 (1973).
7. G. Chesshire and D. Henshaw, *J. Comput. Phys.* **90,** 1 (1990).
8. M. Ciment, *Math. Comput.* **114,** 219 (1971).
9. M. Ciment, *Math. Comput.* **9,** 695 (1972).
10. D. K. Clarke, M. D. Salas, and H. A. Hassan, *AIAA J.* **24,** 353 (1986).
11. C. Corre, K. Khalfallah, and A. Lerat, ''An Efficient Relaxation Method for a 3-D Centered Euler Solver,'' in *Proc. 5th Intern. Symp. CFD, Sendai* (*Japan*), Vol. 1, *1993,* p. 122.
12. R. Enander, Dept. of Scientific Computing, Report No. 112, Uppsala University, March 1990 (unpublished).
13. F. Fezoui and B. Stoufflet, *J. Comput. Phys.* **1,** 174 (1989).
14. M. Goldberg and E. Tadmor, *Math. Comput.* **32,** 1097 (1978).
15. M. Goldberg and E. Tadmor, *Math. Comput.* **36,** 603 (1981).
16. B. Gustafsson, *J. Comput. Phys.* **48,** 270 (1982).
17. B. Gustafsson, ''The Euler and Navier–Stokes Equations. Wellposedness, Stability and Composite Grids,'' in *Computational Fluid Dynamics,* von Karman Institute for Fluid Dynamics, Lecture Series 1991-01, February 18–22, 1991 (unpublished).
18. B. Gustafsson, H.-O. Kreiss, and A. Sundström, *Math. Comput.* **26,** 649 (1972).
19. O. Hassan, K. Morgan, and J. Peraire, AIAA Paper-89-0363, 1989 (unpublished).
20. C. J. Hwang and S. J. Wu, *J. Comput. Phys.* **102,** 98 (1992).
21. A. Jameson, T. J. Baker, and N. P. Weatherill, AIAA Paper 86-0103, 1986 (unpublished).
22. D. E. Keyes, ICASE Report No. 92-44, 1992 (unpublished).
23. K. Khalfallah, G. Lacombe, A. Lerat, A. Raulot, and Z. N. Wu, ''Implicit Multidomain Calculation of Viscous Transonic Flows without Artificial Viscosity or Upwinding,'' in *Computational Fluid Dynamics' 92,* Vol. 2, edited by Ch. Hirsh *et al.* (Elsevier Sci., New York, 1992), p. 675.
24. K. Khalfallah, G. Lacombe, and A. Lerat, *Comput. Fluids* **22,** 381 (1993).
25. H.-O. Kreiss, ''Difference Approximations for the Initial-Boundary Value Problem for Hyperbolic Differential Equations,'' in *Numerical Solution of Nonlinear Differential Equations* (Wiley, New York, 1966), p. 141.
26. H.-O. Kreiss, *Math. Comput.* **22,** 703 (1968).
27. H.-O. Kreiss, AGARD Lecture Series, Vol. 73 (NATO, Neuilly sur Seine, France, 1975), p. 4.1.
28. A. Lerat and J. Sides, ''Efficient Solution of the Steady Euler Equations with a Centred Implicit Method,'' in *Numerical Methods for Fluid Dynamics III,* edited by K. W. Morton and M. J. Baines (Clarendon Press, Oxford, 1988), p. 65.
29. A. Lerat and Z. N. Wu, ''A Subdomain Matching Condition for Implicit Euler Solvers,'' in *Numerical Methods for Fluid Dynamics IV,* edited by M. J. Baines and K. W. Morton, (Clarendon Press, Oxford, 1993), p. 285.
30. D. J. Mavriplis, *AIAA J.* **26,** 824 (1988).
31. D. Michelson, *Math. Comput.* **40,** 1 (1983).
32. R. A. Mitcheltree, M. D. Salas, and H. A. Hassan, *AIAA J.* **26,** 754 (1988).
33. K. Morinishi, *Comput. Fluids* **21,** 331 (1992).
34. J. Oliger, *Math. Comput.* **30,** 724 (1976).
35. S. Osher, *Math. Comput.* **23,** 235 (1969).
36. S. Osher, *Trans. Amer. Math. Soc.* **137,** 177 (1969).
37. S. Osher, *Math. Comput.* **26,** 13 (1972).
38. J. Quirk, *Comput. Fluids* **23,** 125 (1994).
39. E. Pärt-Enander and B. Sjögreen, Dept. of Scientific Computing Report No. 131, Uppsala University, January 1991 (unpublished).
40. E. Pärt-Enander and B. Sjögreen, *Comput. Fluids* **23,** 551 (1994).
41. M. M. Rai, *J. Comput. Phys.* **62,** 472 (1986).
42. M. M. Rai, *Comput. Fluids* **14,** 295 (1986).
43. G. Starius, *Numer. Math.* **35,** 241 (1980).
44. J. L. Steger and J. A. Benek, *Comput. Meth. Appl. Mech. Eng.* **64,** 301 (1987).
45. J. Strikwerda, *J. Comput. Phys.* **34,** 94 (1980).
46. M. Thuné, Dept. of Scientific Computing Report No. 106, Uppsala University, December 1986.
47. M. Thuné, *SIAM J. Sci. Stat. Comput.* **7,** 959 (1986).
48. L. M. Trefethen, *J. Comput. Phys.* **49,** 199 (1983).
49. L. M. Trefethen, *Commun. Pure Appl. Math.* **37,** 329 (1984).
50. L. M. Trefethen, *Math. Comput.* **45,** 279 (1985).
51. J. M. Varah, *SIAM J. Numer. Anal.* **8,** 598 (1971).
52. Z. N. Wu, ''Steady Transonic Flow Computations Using Overlapping Grids,'' in *14th Int. Conf. Numer. Meth. Fluid Dyn., July 11–15, 1994, Bangalore, Inde.* Springer-Verlag, to appear.
53. Z. N. Wu, *SIAM J. Numer. Anal.* **33**(4), to appear.